2015•2016
FACULTEIT GENEESKUNDE EN LEVENSWETENSCHAPPEN
master in de biomedische wetenschappen

Masterproef

Characterization of a new rat model for the cardio-renal syndrome

Promotor :
Prof. dr. Quirine SWENNEN

Laura Blockken

Scriptie ingediend tot het behalen van de graad van master in de biomedische wetenschappen

De transnationale Universiteit Limburg is een uniek samenwerkingsverband van twee universiteiten in twee landen: de Universiteit Hasselt en Maastricht University.

universiteit hasselt
KNOWLEDGE IN ACTION

Universiteit Hasselt | Campus Hasselt | Martelarenlaan 42 | BE-3500 Hasselt
Universiteit Hasselt | Campus Diepenbeek | Agoralaan Gebouw D | BE-3590 Diepenbeek

universiteit hasselt | Maastricht University

2015•2016
FACULTEIT GENEESKUNDE EN LEVENSWETENSCHAPPEN
master in de biomedische wetenschappen

Masterproef

Characterization of a new rat model for the cardio-renal syndrome

Promotor :
Prof. dr. Quirine SWENNEN

Laura Blockken
Scriptie ingediend tot het behalen van de graad van master in de biomedische wetenschappen

universiteit hasselt | Maastricht University

Table of contents

Abbreviations

ADHERE	acute decompensated heart failure national registry
ADQI	acute dialysis quality initiative
AHA	American heart association
AKI	acute kidney injury
ANP	A-type natriuretic peptide
AUC	area under the curve
AWT	anterior wall thickness
α-SMA	α-smooth muscle actin
BNP	B-type natriuretic peptide
CK	creatinine kinase
CNP	C-type natriuretic peptide
CO	cardiac output
CRS	cardio-renal syndrome
cTn	cardiac troponin
cTnC	cardiac troponin C
cTnI	cardiac troponin I
cTnT	cardiac troponin T
CVP	central venous pressure
Cys C	cystatin C
DPX	distyrene plasticizer xylene
EDV	end-diastolic volume
EDTA	ethylenediaminetetraacetic acid
EF	ejection fraction
ESC	european society of cardiology
ESV	end-systolic volume
FENa	fractional sodium excretion
FS	fractional shortening
GFR	glomerular filtration rate
HF	heart failure
HR	heart rate
H&E	hematoxylin and eosin
IAP	intra-abdominal pressure
IL	interleukin
KIM-1	kidney injury molecule-1
LV	left ventricle
LVEDD	left ventricle end-diastolic diameter
LVEDV	left ventricle end-diastolic volume
LVESD	left ventricle end-systolic diameter
LVESV	left ventricle end-systolic volume
LVP	left ventricular pressure
NADPH	nicotinamide adenine dinucleotide phosphate

NGAL	neutrophil gelatinase-associated lipocalin
NP	natriuretic peptide
PBS	phosphate buffered saline
PCT	proximal convoluted tubule
PFA	paraformaldehyde
PWT	posterior wall thickness
RAAS	renin-angiotensin-aldosterone system
RM	repeated measures
ROC	receiver operating characteristic
ROS	reactive oxygen species
SNS	sympathetic nervous system
SV	stroke volume
TGF-β1	transforming growth factor-β1
VCI	vena cava inferior
ZOL	Ziekenhuis Oost-Limburg
2D	two dimensional

Acknowledgements

This thesis is the result of an extensive training as master student Biomedical Sciences at the Biomedical Research Institute (BIOMED) in Diepenbeek. Without the help of certain people, it would not be possible to succeed in and profit from this broad experience. Therefore, I would like to thank a few people.

I would like to express my gratitude to prof. dr. Quirine Swennen for offering me this wonderful position as senior intern in the cardiology group of BIOMED. Prof. Swennen was always ready to answers my questions and to help me with every aspect of my thesis. In addition, drs. Jirka Cops was my approach for all the practical issues I encountered in the laboratory or with animal work every minute of the day. She was also my point of return to discuss problems and results. Both of my supervisors were not only motivated and enthusiastic mentors in this journey, but also people to whom I could talk about matter of all sort. My sincere thanks also goes out to my second examiner, dr. Annelies Bronckaers, for her advice and suggestions during this project.

This thesis would not be complete without the expertise and help of different people. Therefore, I would like to thank prof. dr. Virginie Bito and dr. Vesselina Ferferieva for sharing their experience and knowledge, especially with the echocardiographic analyses. For the analyses of the urine and blood samples, I am grateful for the help of prof. dr. Joris Penders and Carmen Reynders of the clinical laboratory in the hospital Ziekenhuis Oost-Limburg (ZOL). Additionally, I would like to thank all other people in BIOMED, who helped me with their expertise and knowledge in one way or another.

I would also like to thank my fellow students for their support during this journey. Last, I would like to show my appreciation to my family and friends for letting me have this opportunity and experience in obtaining my master diploma Biomedical Sciences. They were my greatest motivators and supporters throughout these years.

Summary

Introduction: The cardio-renal syndrome (CRS) is an umbrella term for life-threatening diseases in which cardiac and renal dysfunction occur simultaneously. It has been shown that heart failure patients with an increase in intra-abdominal and central venous pressure (CVP), indicating the presence of abdominal and venous congestion, have a higher risk to develop CRS due to worsening renal function. However, it is unclear how abdominal venous congestion in itself contributes to CRS. It is hypothesized that abdominal venous congestion impairs heart and kidney function by causing damage to the heart and kidneys.

Materials and methods: Male Sprague-Dawley rats were subjected to sham-operation (n = 6) or thoracic vena cava inferior (VCI)-constriction (n = 7). Bodyweight, plasma and urine samples and echocardiographic data were acquired at baseline and during a twelve-week follow-up period. Plasma and urine samples were investigated for different standard clinical parameters to evaluate heart, kidney and liver function. Hemodynamic measurements and organ weights were obtained at the end of the study in week 12. Heart, kidney and liver tissues were used to measure morphological changes including cardiac wall thickness, width of Bowman's space and hepatocyte hypertrophy, respectively. The percentage fibrosis was also determined in these tissues.

Results: The hemodynamic measurements showed an increase in abdominal CVP after VCI constriction. This increase had no effect on bodyweight and organ weight normalized to tibia length, except for an increase in spleen weight. The hemodynamic measurements in the left ventricle, echocardiographic parameters and creatine kinase activity levels showed no change in cardiac function after VCI constriction. On the other hand, kidney function was minimally affected by VCI constriction as plasma creatinine, cystatin C, chloride and sodium levels were increased in the VCI group, but urinary creatinine, creatinine clearance, urinary chloride, sodium and total protein levels were not influenced by VCI constriction. Liver function deteriorated as plasma bilirubin levels were increased after VCI constriction. However, only the kidney showed morphological changes after VCI constriction as the width of Bowman's space was increased while cardiac wall thickness and hepatocyte hypertrophy were unchanged in the VCI group. The percentage fibrosis was only increased in liver tissue sections after VCI constriction and not in the heart and kidneys.

Discussion and conclusions: The rat model is validated as abdominal venous congestion was induced via constriction of the VCI. As the effect of the VCI constriction on heart and kidney function was limited, the presence of abdominal venous congestion was insufficient to induce CRS. Consequently, in future CRS research, the role of abdominal venous congestion in CRS development and progression can be further explored by combining this rat model with other models of heart or kidney failure.

Samenvatting

Introductie: Het cardio-renaal syndroom (CRS) is een overkoepelende term voor levensbedreigende ziektes waarin hart- en nierfalen simultaan aanwezig zijn. Het is aangetoond dat hartfalen patiënten met een verhoogde intra-abdominale druk en centraal veneuze druk (CVD), wat duidt op de aanwezigheid van abdominale en veneuze congestie, een verhoogde kans hebben om CRS te ontwikkelen doordat de nierfunctie verslechtert. Het is echter niet duidelijk hoe abdominale veneuze congestie bijdraagt tot CRS. De hypothese is dat abdominale veneuze congestie de hart- en nierfunctie verslechtert door het hart en de nieren te beschadigen.

Materiaal en methoden: Mannelijke Sragues-Dawley ratten werden onderworpen aan éénzelfde operatie met (n = 7) of zonder (n = 6) thoracale vena cava inferior (VCI)-constrictie. Lichaamsgewicht, plasma en urine stalen en echocardiografie data werden verzameld voor de operatie en gedurende een periode van twaalf weken na de operatie. Plasma en urine stalen werden onderzocht voor verschillende standaard klinische parameters om hart-, nier- en leverfunctie te onderzoeken. Hemodynamische metingen en orgaangewichten werden verkregen aan het einde van de studie in week 12. Morfologische veranderingen werden gemeten in hart-, nier- en leverweefsel: hartwanddikte, de grootte van de ruimte van Bowman en levercel hypertrofie, respectievelijk. Het percentage fibrose werd ook bepaald in deze weefsels.

Resultaten: De hemodynamische metingen toonden een verhoging in CVD na VCI constrictie. Lichaamsgewicht en orgaangewichten genormaliseerd ten opzichte van tibialengte waren onveranderd, met uitzondering van een zwaardere milt in de VCI groep. De hemodynamische metingen, echocardiografie parameters en creatine kinase activiteit toonden geen verandering in hartfunctie na VCI constrictie. Aan de andere kant, nierfunctie werd minimaal beïnvloed door VCI constrictie aangezien plasma creatinine, cystatin C, natrium en chloor levels verhoogd waren. Urinair creatinine, creatinine klaring, urinair chloor, natrium en totaal proteïn waren echter onveranderd in de VCI groep. Leverfunctie verslechterde na VCI constrictie wat weerspiegeld werd in verhoogde plasma bilirubine levels. Alleen de nier vertoonde morfologische veranderingen aangezien de grootte van de ruimte van Bowman verhoogd was, terwijl hartwanddikte en levercel hypertrofie niet beïnvloed waren door de VCI constrictie. Het percentage fibrose was enkel verhoogd in leverweefsel na VCI constrictie en niet in hart- en nierweefsel.

Discussie en conclusies: Het rat model is gevalideerd omdat abdominale veneuze congestie werd geïnduceerd via VCI constrictie. De aanwezigheid van abdominale veneuze congestie was niet voldoende om CRS te induceren aangezien het effect van VCI constrictie gelimiteerd was op hart- en nierfunctie. Bijgevolg kan toekomstig onderzoek de rol van abdominale veneuze congestie in de ontwikkeling en progressie van CRS verder onderzoeken door dit rat model te combineren met andere modellen van hart- of nierfalen.

1 Introduction

Heart failure (HF) and kidney dysfunction often occur simultaneously in patients because of an interdependence between heart and kidney function. This interdependence increases the complexity of heart and kidney pathologies and leads to adverse outcomes for patients, which has major health and economic implications for society worldwide (1, 2). The Acute Decompensated Heart Failure National Registry (ADHERE) showed that 30% of HF patients have worsening renal function (3). The American Heart Association (AHA) estimated in 2015 that 5.7 million Americans were confronted with HF and it was predicted that this number will increase to more than 8 million people in 2030. This corresponds with a total cost of 30,7 billion dollars (or 23 billion euros) for HF patients in 2012 and an increase to 69,7 billion dollars (or 52,2 billion euros) by 2030 in America (4). Similar numbers were obtained by the European Society of Cardiology (ESC) for Europe in 2008 (5). As 30% of these numerous HF patients are also diagnosed with kidney dysfunction, the costs for the society increases because of a more complex treatment of these patients. Consequently, a better knowledge of the interdependence between heart and kidney function is essential to improve patient outcomes by developing new therapeutic strategies. This will also lead to a reduction in medical costs associated with the treatment of these patients.

1.1 The cardio-renal syndrome

The interaction between the heart and kidneys in a dysfunctional state is assembled in one unifying term: the cardio-renal syndrome (CRS) (1). The cardio-renal syndrome is an umbrella term for life-threatening disorders in which cardiac and renal dysfunctions occur simultaneously. This group of conditions is more precisely defined by the Acute Dialysis Quality Initiative (ADQI) as 'disorders of the heart and kidneys whereby acute or chronic dysfunction in one organ may induce acute or chronic dysfunction in the other' (6).

Five different subtypes of CRS are established in order to include all possible disorders that are defined by CRS. This subdivision is based on whether the heart or kidneys are primarily dysfunctional and whether this dysfunction is acute, chronic or secondary (Table 1). Type 1 CRS is described as an acute cardio-renal syndrome in which sudden deterioration of cardiac function leads to acute kidney injury. Type 2 CRS is characterized by chronic dysfunction of the heart causing chronic kidney disease and is defined as a chronic cardio-renal syndrome. In contrast, type 3 CRS is outlined as an acute reno-cardiac syndrome in which abrupt impairment of renal function leads to acute cardiac disorders. Type 4 CRS is manifested by chronic kidney disease causing a chronic decline in heart function and is described as a chronic reno-cardiac syndrome. Finally, type 5 CRS is delineated as a secondary cardio-renal syndrome in which a systemic condition (e.g. sepsis, diabetes mellitus,…) causes both cardiac and renal dysfunction (6). It is hard to distinguish the five different subtypes of CRS because the classification does not depend on pathophysiologic characteristics, but on etiologic and chronologic interactions between the heart and kidneys (7). Another challenge is the possibility that patients may transit from one type of CRS to another (e.g. a transition between type 1 and 2) (6).

Table 1: Different subtypes of the cardio-renal syndrome.

CRS	Syndrome	Primary dysfunction	Secondary dysfunction	Time frame
Type 1	Cardio-renal	Heart	Kidney	Acute
Type 2	Cardio-renal	Heart	Kidney	Chronic
Type 3	Reno-cardiac	Kidney	Heart	Acute
Type 4	Reno-cardiac	Kidney	Heart	Chronic
Type 5	Secondary	Systemic condition	Heart and kidney	Acute or chronic

The cardio-renal syndrome is divided in five different subtypes in order to include all possible disorders defined by CRS. This subdivision is based on the primary dysfunctional organ (heart or kidney) and the time frame of this dysfunction (acute or chronic). In exception, in type 5 CRS the primary dysfunction is a systemic condition (e.g. sepsis) the cause of heart and kidney failure. Adapted from Ronco C. *et al*., 2009 (6).

1.2 Pathogenesis of CRS

The bi-directional relationship between the heart and kidneys is determined by different regulatory mechanisms, including hemodynamic, (neuro)hormonal and biochemical components. More specifically, renin-angiotensin-aldosterone system (RAAS) and sympathetic nervous system (SNS) activation and oxidative stress play a role in the pathogenesis of CRS (7). These cause structural and functional damage to the heart and kidneys and lead to heart and kidney dysfunction contributing to CRS development and progression (8).

1.2.1 Hemodynamic alterations

It is suggested that several hemodynamic alterations can contribute to CRS: a decrease in cardiac output (CO), venous congestion and an increase in intra-abdominal pressure (IAP) (8). Initially, it was thought that CRS was the consequence of a reduced CO, which impaired renal function due to a lowered perfusion of the kidneys. However, a decrease in CO can not be the sole contributor to CRS because only a small number of CRS patients show a reduction in CO (7, 8). Another possible culprit in CRS pathogenesis is venous congestion, which is caused by overfilling or distention of the veins by blood. This is measured as an increase in the pressure of the thoracic vena cava near the right atrium, also called the central venous pressure (CVP) (9). As shown by Winton F.R. *et al*. (1931), elevated CVP leads to kidney dysfunction by diminishing renal perfusion and glomerular filtration rate (GFR) (10). Data of HF patients demonstrated that venous congestion (rather than decreased CO) is the most important hemodynamic factor in CRS development and progression by worsening renal function (9). Finally, an increase in IAP could contribute to CRS as approximately 60% of HF patients with an increase in IAP have a deteriorating renal function (11, 12). In addition, it is demonstrated that a reduction in IAP by mechanical fluid removal in these patients improves renal function (13). Intra-abdominal pressure is the steady state pressure in the abdominal cavity and is used as a measure for abdominal congestion (14). This implies a role for abdominal congestion in the development and progression of CRS. Abdominal congestion is more precisely defined as congestion in the spleen, the veins and interstitium (15).

This project will focus on the role of abdominal CVP in CRS development and progression. It has been shown in other disease settings (intra-abdominal hypertension in pigs and rats and burn victims) that CVP is positively correlated to IAP (16, 17). This correlation will be referred to as abdominal CVP and the congestion following from this increase in abdominal CVP is termed abdominal venous congestion. The following paragraphs will give an literature overview on how an

increase in CVP and IAP contribute to renal and other derangements, which will clarify the possible role of increased abdominal CVP in CRS development and progression.

1.2.1.1 Renal derangements

It is postulated that renal function deteriorates as a consequence of an increase in CVP caused by compression of the vena cava inferior (VCI) in case of abdominal congestion. The increased CVP is transmitted back to the renal veins and causes an increase in renal venous pressure. Additionally, the kidneys are directly compressed by an increase in IAP (18, 19). These effects lead to worsening renal function by development of renal ischemia because of a decreased renal perfusion (12). The increase in CVP also results in distention of the venules surrounding the distal end tubules, which leads to compression of the tubule lumen. This is in turn the cause for a decrease in GFR and urine production (10). Via these mechanisms, it is thought that renal function declines in the presence of increased abdominal CVP.

1.2.1.2 Other derangements

In the literature, some assumptions are being made on how abdominal congestion is supported by derangements in the abdominal compartment. Abdominal congestion might be the result of malfunctioning splanchnic capacitance veins, which normally store and release blood to regulate the effective circulatory volume (20). When these veins malfunction, there is an undesired shift in blood from the effective circulatory volume to the splanchnic vasculature, supporting splanchnic congestion (15, 21).

Additionally, alterations in liver, spleen and gut function due to abdominal congestion could further promote abdominal congestion. First, blood flow to the liver is decreased because of hepatic portal vasoconstriction and excessive vasodilation of the splanchnic vascular system, which leads to perceived hypovolemia. This triggers a reflex in which activation of hepatic nerves leads to stimulation of renal nerves (the hepato-renal reflex). As a result, renal vasoconstriction and sodium retention is promoted (15, 22). Second, the spleen is part of the splanchnic vasculature and helps in alleviating splanchnic congestion by increasing lymph efflux. However, continuous lymph efflux also leads to perceived hypovolemia, which in turn causes an increase in fluid retention due to neurohumoral stimulation (15, 23). Third, abdominal congestion causes an increase in secretion of gut-derived hormones and changes in intestinal morphology and function (15, 24). These gut-derived hormones influence sodium homeostasis, while toxins (mainly from micro-organisms, e.g. lipopolysaccharides) escape from the gut into the circulation and further contribute to cardiac and renal dysfunction by stimulating systemic inflammation (15, 25).

Outside the abdominal compartment, an increase in IAP is transdiaphragmatically transmitted back to the thorax, which leads to increased intrathoracic pressures. This causes a decrease in venous return by compression of the VCI further exacerbating abdominal congestion (13, 26). It should be noted that these are only assumptions. More research is necessary to elucidate the precise mechanisms contributing to these derangements and their role in the development and progression of CRS due to abdominal congestion.

1.2.2 (Neuro)hormonal changes

The RAAS and SNS both play a role in maintaining cardiac and renal function in balance. A decrease in arterial filling pressure leads to a decrease in renal perfusion and delivery of sodium and chloride. These changes are sensed by baroreceptors, macula densa cells and juxtaglomerular cells. Next, the RAAS and SNS are activated, which stimulates vasoconstriction and sodium and water retention as a compensation for the decrease in arterial filling pressure. The disadvantage of this compensation is the development of congestion because of a volume overload or volume misdistribution (1, 7, 12). The SNS also enhances RAAS activation via stimulation of renin release from glomerular cells. Chronic activation of these systems leads to inflammation, fibrosis, increased oxidative stress and endothelial dysfunction in the heart and kidneys, which all contribute to CRS (7, 27).

1.2.3 Oxidative stress

There is ever growing evidence indicating a role for oxidative stress in CRS. Activation of previously mentioned (neuro)hormonal systems are strong stimulators for oxidative injury leading to endothelial dysfunction, inflammation and cell death in the heart and kidneys (12). Especially, nicotinamide adenine dinucleotide phosphate (NADPH) oxidase seems to play an important role in these processes. Nicotinamide adenine dinucleotide phosphate oxidase is activated via angiotensin II of the RAAS and is involved in cardiac and renal dysfunction by increasing reactive oxygen species (ROS) production (28, 29). These mechanisms are mainly demonstrated in heart and kidney failure separately. Consequently, it is reasoned that oxidative stress also plays a role in CRS via these mechanisms (30). However, research focusing on this particular part is limited in CRS.

1.3 Diagnosis and biomarkers

Diagnosis of deteriorating heart and kidney function is essential in the prevention and treatment of CRS. Currently, HF diagnosis is based on signs and symptoms displayed by the patient (e.g. breathlessness, fatigue,…), which are mostly the consequence of sodium and water retention. The presence of congestion is checked by distention of the jugular vein (increased CVP), ankle swelling (peripheral edema), organ enlargement, etc. Additionally, cardiac dysfunction in HF patients is investigated by electrocardiography and laboratory tests including natriuretic peptides (discussed in 1.3.2). Finally, concomitant renal dysfunction is assessed by measuring serum creatinine levels (>1,7 mg/dl) and creatinine clearance (<60 ml/min) (31).

The current strategy delays diagnosis of CRS and thereby limits prevention and treatment of CRS. Consequently, the possibility for early diagnosis is of great importance. This can be achieved by measuring a panel of cardiac and renal biomarkers since heart and kidney dysfunction occur simultaneously in CRS. A biomarker should be clinically measurable, add new information and help the clinician to manage patients (32).

1.3.1 Renal biomarkers

Currently available tests are unable to timely diagnose renal injury. Serum creatinine, as a marker of GFR, is not suitable to diagnose renal tubular injury when there is no immediate reduction in GFR after injury. Therefore, other biomarkers are necessary to confirm kidney damage (33).

First, neutrophil gelatinase-associated lipocalin (NGAL) is one of the most promising biomarkers for acute kidney injury (AKI) and can be measured in blood and urine (34). It is normally expressed at very low levels but expression is markedly increased after epithelial injury (35). Increased blood NGAL levels have been shown to be a sensitive biomarker of renal dysfunction in chronic HF patients with normal serum creatinine levels but reduced GFR (36). Second, cystatin C (cys C) is freely filtered by the glomerulus, reabsorbed and catabolized completely by proximal convoluted tubule (PCT) and not actively secreted in the urine. It can be measured in the serum and in the urine to predict AKI. Cystatin C levels rise in the urine as cys C is less reabsorbed after damage to the PCT, but also increase in the serum as GFR is decreased (35, 37). As cys C and NGAL can both be measured in urine and blood, these biomarkers have the advantage that fractional excretion can be calculated. If only the urinary concentration of these biomarkers could be measured, the concentration would vary with water reabsorption while fractional excretion takes GFR into account via creatinine clearance. Third, IL-18 is a pro-inflammatory cytokine overexpressed in the PCT after renal injury. However, there are non-conclusive results for urinary IL-18 predicting AKI (33). Last, kidney injury molecule 1 (KIM-1) is also overexpressed in PCT after AKI and increased levels of KIM-1 can be measured in the urine (38). Elevated urinary KIM-1 can be detected before a rise in serum creatinine and has significant prognostic value for patients with AKI (33, 39).

1.3.2 Cardiac biomarkers

Cardiac biomarkers are measured as an indication of heart injury. The main focus of cardiac biomarkers is directed at the natriuretic peptides (NP). These are released by cardiomyocytes in response to wall stress from intravascular volume expansion, increased atrial and systemic pressure and increased ventricular mass. Natriuretic peptides compensate for an imbalance in hemodynamic parameters by promotion of natriuresis, vascular smooth muscle cell relaxation and direct myocardial effects (e.g. inhibition of cardiac cell death and reduction of hypertrophy and fibrosis) (33, 40, 41). There are three types of NPs: A-type, B-type and C-type. A-type natriuretic peptide (ANP) and B-type natriuretic peptide (BNP) are synthesized and secreted in response to increased wall stress. On the other hand, C-type natriuretic peptide (CNP) is only released by cardiac tissue in minimal amounts (33). B-type natriuretic peptide levels are included in laboratory tests for the diagnosis and exclusion of HF. B-type natriuretic peptide can also be used as predictors of mortality and non-fatal cardiac events, but also to give an indication on the effectiveness of the therapeutic approach (42). However, it should be kept in mind that NP levels could also be elevated in other clinical situations than HF (e.g. asthma, acute ischemia,…) (33).

Cardiac troponins (cTns) are also cardiac biomarkers and are released by the heart in response to myocardial injury (43). Troponins are involved in the contraction of striated muscle and are composed of three different subunits; cardiac troponin C (cTnC), cardiac troponin I (cTnI) and cardiac troponin T (cTnT). Troponin T stabilizes the cTnC/cTnI complex and subsequent binding of Ca^{2+} to cTnC causes cTnI to be released from actin, which allows binding of myosin to actin and results in contraction (44). For diagnostic use, there are two main troponins investigated as possible biomarkers, i.e. cTnT and cTnI. Although there still is some controversy, cTns could be used in the prediction of cardiac events and mortality stratification in patients with renal dysfunction (43, 45).

1.3.3 Panel of biomarkers

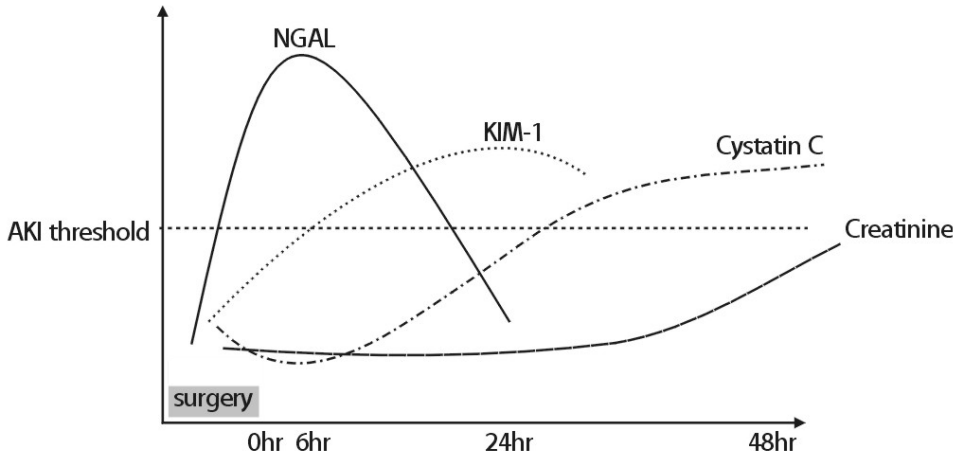

Figure 1: Schematic representation of the changes in urinary or serum biomarkers levels for the detection of AKI after cardiac surgery. After cardiac surgery, urinary NGAL levels rapidly increase and peak at six hours, while urinary KIM-1 gradually increases and peaks at 24 hours after surgery. On the other hand, serum cystatin C and creatinine only steadily increase after 24 hours after surgery. AKI, acute kidney injury; NGAL, neutrophil gelatinase-associated lipocalin; KIM-1, kidney injury molecule-1. Adapted from Lee *et al.*, 2012 (43).

Biomarkers have varying expression levels at different time points after an insult (Figure 1). For renal biomarkers, it seems that urinary NGAL and KIM-1 are early biomarkers, while serum cys C and creatinine levels only increase after 24h. On the other hand, cardiac biomarkers are continuously expressed after cardiac surgery and can be measured as an indication of injury but also as an approach to assess treatment strategies. Therefore, it is necessary to include multiple renal and cardiac biomarkers in clinical tests for optimal evaluation of heart and kidney damage (33). By measuring these biomarkers, an early diagnosis can be made and a preventive or more specific therapy can be started, which is beneficial for the patient.

1.4 Therapies

Since congestion is one of the most frequent reasons for expensive hospital admissions with HF patients, efficient management and relieve of congestion is of great importance (3, 46). However, CRS is a multifaceted disorder, which complicates therapy. Current therapeutic approaches use a combination of different drugs to relieve congestion while it is suggested that in the future more patient specific treatments could prove beneficial (46).

1.4.1 Current therapies

In HF patients, the main goal is to maintain a neutral sodium balance and to avoid volume overload or misdistribution. Current treatment regimens contain RAAS blockers, β-blockers (SNS blockers) and mineralocorticoid receptor antagonists (aldosterone inhibitor) because of the evidence indicating a role for these neurohumoral players in developing congestion (as described in 1.2.2) (27, 31). Additionally, congestion could be relieved by dietary salt restriction as congestion is accompanied by an increased sodium retention (46).

Furthermore, diuretics are used to reduce volume overload by stimulating diuresis or natriuresis. First, loop diuretics work by directly inhibiting the $Na^+/K^+/2Cl^-$-symporter on the luminal membrane of tubule cells at the loop of Henle to decrease chloride reabsorption resulting in natriuresis.

However, this decreased chloride reabsorption is also sensed by macula densa cells, which leads to distal tubular cell hypertrophy and RAAS and SNS activation (46, 47). In other words, the use of loop diuretics is associated with adverse outcomes (e.g. worsening renal function) but also loop diuretic resistance (48). This can be avoided by the combinatorial use of loop and thiazide diuretics (49). Thiazide diuretics decrease salt reabsorption by inhibiting the Na-Cl cotransporter in the distal convoluted tubule of the kidney (47). Other frequently used diuretics are carbonic anhydrase inhibitors that block sodium bicarbonate reabsorption in the proximal tubules, which results in a higher delivery of sodium and chloride to the macula densa cells. This leads to a reduction in neurohumoral activation and thereby water and salt retention (46, 50). Additionally, diuresis can also be stimulated by administrating vasopressin antagonists. Normally, vasopressin is secreted as a response to angiotensin II release due to RAAS activation and stimulates water reabsorption by the incorporation of aquaporin-2 in collecting duct cells of the nephron. By inhibiting aquaporin-2 incorporation with vasopressin antagonists, diuresis is stimulated without influencing sodium excretion (46).

On the other hand, it has been shown in different clinical trials that abdominal congestion can be relieved by mechanical fluid removal, resulting in improved renal function. This is mostly applied when patients do not respond to or are resistant for diuretics (31). First, congestion of the interstitium can be diminished by paracentesis, in which fluid is removed from the abdomen via a drain to a container (13). Second, mechanical fluid removal through ultrafiltration reduces interstitial congestion more efficiently compared to diuretics. Ultrafiltration is a process in which solutes are exchanged from the blood to a solution with known solute concentrations through a semi-permeable membrane. However, the need for central venous access is associated with severe complications (e.g. hemorrhage and bacterial infections) (51, 52). As an alternative, continuous ambulatory peritoneal dialysis can be performed in HF patients with renal dysfunction, which is ultrafiltration of peritoneal fluid. This has the advantage of slow ultrafiltration, which has minimal impact on hemodynamics and thereby neurohumoral activation (15, 53).

1.4.2 Future therapies

New therapies to avoid volume overload and to maintain a normal sodium balance are already being tested in clinical trials. First, it may be possible to regulate sodium balance by the use of natriuretic agents or sodium binders. These natriuretic agents have been shown to stimulate natriuresis by decreasing renal sodium avidity (46, 54). On the other hand, sodium binders prevent both sodium and water retention. Clinical trials showed that oral sodium binders trap water and sodium in the gut and eliminate water through the feces without causing electrolyte imbalances. As a result, hemodynamics are unaffected, which makes sodium binders advantageous to natriuretic agents as they do not further activate neurohumoral pathways. This may provide an alternative route in the presence of renal dysfunction to control volume overload that does not involve the kidney (46, 55, 56). Second, vasodilator therapy can lower the need for diuretics to treat volume overload. This may be the result of improved systemic and renal hemodynamics, which causes better renal perfusion. In other words, vasodilator therapy helps in a redistribution of volume by recruiting venous capacitance veins or by increasing the effective circulatory volume filtrated by the kidneys. Additionally, vasodilation relaxes the peripheral arteries reducing left ventricular

afterload, which results in lowered ventricular wall stress. This therapy can prove useful in patients with a high systemic vascular resistance and low CO (46). Finally, renal sympathetic denervation could be a new therapeutic strategy because sympathetic up-regulation is one of the drivers of increased sodium retention (15, 27). However, future research is necessary to investigate the efficacy of these therapies in CRS patients.

1.5 Research plan

As stated previously, this project will focus on the involvement of abdominal venous congestion in the development and progression of CRS. However, patients first present with heart or kidney failure before developing abdominal venous congestion. This impedes our understanding on how abdominal venous congestion in itself contributes to CRS development and progression. It is hypothesized that abdominal venous congestion affects heart and kidney function by causing damage to these organs. Therefore, a new animal model of abdominal venous congestion will be used to investigate the effects of abdominal venous congestion on heart and kidney function.

For the moment, animal models of heart and kidney failure are available for CRS research. However, induction of failure in one organ does not always induce reproducible dysfunction in the other. To solve this problem researchers combine animal models of heart and kidney failure to investigate CRS pathology. This combination is unable to show that combined renal and cardiac injury causes additive damage to both organs (57). Additionally, patients first present with dysfunction in one organ before developing dysfunction in the other. In other words, heart and kidney dysfunction rarely develops simultaneously. Therefore, the combination of these different models is not representative for the human situation.

Consequently, during this project, a rat model of abdominal venous congestion will be developed. In the future, this model can be used in combination with other models of heart or kidney failure. This will create a more realistic analogy with the human situation. Abdominal venous congestion is achieved in rats by constricting the thoracic VCI, which will lead to an increase in the pressure below this constriction. In this project, the constriction will be made cranial of the confluence of the vena hepatica and above the diaphragm. The rats will also be studied in a follow-up period of twelve weeks in order to assess short and long term effects of VCI constriction on heart and kidney function.

To investigate these effects, the first objective is the validation of the rat model for abdominal venous congestion by performing hemodynamic measurements above and below the constriction. Next, the effects of abdominal venous congestion on heart and kidney function will be investigated *in vivo*. After sacrifice of the rats, heart and kidney tissue will be evaluated by different *in vitro* experiments. It is expected that these data will give an indication on how abdominal venous congestion influences heart and kidney function.

2 Materials and methods

2.1 Animals

All experiments were approved by the local ethical committee of Hasselt University and were performed according to the guidelines described in directive 2010/63/EU on the protection of animals used for scientific purposes. Rats were housed in a conventional animal facility at Hasselt University under controlled conditions; room temperature at ± 22°C, a light-dark schedule of 12/12h and food and water *ad libitum*. In every cage, two or three rats were group-housed with bedding material and cage enrichment. Before the start of the study, rats were allowed to acclimatize for several days after arrival and were handled daily for two weeks to reduce handling-induced stress.

2.2 Experimental planning

First, ten rats were subjected to sham operation (n = 3) or VCI constriction (n = 4) in a pilot study, resulting in a mortality rate of 30%. These rats were followed up for six weeks (Table 2). Before surgery, bodyweight and blood and urine samples were obtained as baseline measurements. During the following six-week evaluation, bodyweight was monitored consistently every week. In order to provide a recovery period for the rats after surgery, blood samples were obtained in week 2, 4 and 6 and urine samples were obtained in week 5 for further analysis. Afterwards (week 6), hemodynamic measurements were performed and rats were sacrificed due to the invasiveness of this procedure. After organ retrieval, heart, kidney and liver tissues were used for the *in vitro* experiments as explained in the following paragraphs. This pilot study provided some first indications on the validation of the rat model for abdominal congestion and how abdominal congestion influences heart and kidney function. In addition, this pilot study was used to optimize experimental procedures.

Table 2: Planning for the *in vivo* experiments of the pilot study during six weeks.

Week	0	1	2	3	4	5	6
Surgery	■						
Bodyweight	■	■	■	■	■	■	■
Blood samples	■		■		■		■
Urine samples	■					■	
Hemodynamic measurements							■
Sacrifice							■

In the pilot study, rats were followed up for six weeks after surgery. During the six-week evaluation, bodyweight was followed up and urine and blood samples were collected. At the end of week 6, hemodynamic measurements were performed and after this invasive procedure, rats were sacrificed.

Second, a new *in vivo* study was started with twenty rats and an evaluation period of twelve weeks (Table 3). A mortality rate of 35% was achieved with seven rats VCI-constricted and six rats sham-operated. Bodyweight, blood and urine samples and echocardiography were obtained as baseline measurements before surgery. Thereafter, bodyweight was followed up every week and urine and blood samples were obtained in week 3, 6, 9 and 12. Echocardiography was repeated in week 6

and 12. Similar to the pilot study, hemodynamic measurements were performed at the end of the study period and rats were sacrificed.

Table 3: Planning for the *in vivo* experiments during twelve weeks.

Week	0	1	2	3	4	5	6	7	8	9	10	11	12
Surgery													
Bodyweight													
Echocardiography													
Urine and blood samples													
Hemodynamic measurements													
Sacrifice													

The surgery of the rats is the start of the *in vivo* experiments lasting for twelve weeks. During these twelve weeks, the rats were subjected to echocardiography and urine and blood samples were collected. At the end of week 12, hemodynamic measurements were performed and the rats were sacrificed.

2.3 Constriction of the thoracic vena cava inferior

Sprague-Dawley rats (200 – 250g, Charles River, France) were randomly subjected to VCI constriction or sham surgery. For both groups, anesthesia was induced with 3% isoflurane and O_2 at a flow rate of 2 L/min in an induction chamber. Anesthesia was maintained by intubation via a respiratory pump (Inspira asv, Harvard Apparatus, Massachutes) with 1-2% isoflurane. Rats were placed on a heating pad during the entire procedure. Subsequently, a right anterolateral thoracotomy was performed and the VCI was dissected free from the surrounding tissues. A permanent ligature was applied around the VCI with a 6-0 prolene suture (Ethicon, Switzerland) against a 20G needle, which was removed instantly after constriction. The intercostal muscles were joined via interrupted sutures with a 3-0 vicryl suture (Ethicon, Switzerland) and the superficial muscles and skin were closed with a 4-0 ethilon continuous suture (Ethicon, Switzerland). Mechanical ventilation was sustained until full recovery of independent respiration and initiation of spontaneous movement. To further support recovery, the rats were placed on a heating pad with O_2 supply via a face mask. Sham operated rats were subjected to the same procedure except no constriction was applied around the VCI. Metacam (1 mg/kg, Boehringer, Germany) was applied subcutaneously as analgesia 12 – 24h after surgery. As some wounds festered, antibiotics (10 mg/kg/day, Baytril, Bayer, Belgium) were administered via the drinking water for five days. Antibiotics were given to all rats in order to avoid variation between groups due to these antibiotics.

2.4 Echocardiography

To perform transthoracic echocardiography, rats were anesthetized as previously described. Rats were placed on a heating pad and anesthesia was maintained for the entire procedure with 2 - 4% isoflurane. Two dimensional (2D) images (B-mode) were obtained using a 10MHz probe connected to an ultrasound computer (Vivid *i,* GE Healthcare, Diegem, Belgium). The transducer was placed at mid-ventricular level to obtain parasternal long and short axis images. The short axis 2D-images at the mid-papillary level were used to determine the left ventricle (LV) end-diastolic and end-systolic diameter (LVEDD and LVESD) and mean posterior and anterior wall thicknesses (PWT and

AWT) of systole and diastole. Percentage LV fractional shortening (FS%) was calculated with the aid of these parameters: [(LVEDD – LVESD) / LVEDD] x 100. Left ventricle end-systolic and end-diastolic volume (ESV and EDV) was calculated with the following formula $\pi * D_M^2 * B / 6$. D_M was provided by the LVEDD or LVESD, while B is determined by LV length in the long-axis view. Percentage LV ejection fraction (EF%) was calculated by [(EDV – ESV) / EDV] x 100 and stroke volume (SV) via EDV – ESV. Last, M-mode in the short-axis view were used to determine heart rate (HR). Cardiac output was then calculated via the formula (SV * HR) / 1000.

2.5 Plasma and urine samples

Blood was collected via the tail artery in ethylenediaminetetraacetic acid (EDTA) tripotassium salt plasma tubes (Multivette 600 K3E, Sarstedt, Germany) under isoflurane anesthesia as previously explained. Plasma tubes were centrifuged at 2000 rpm for 10 minutes (Micro Star 17R, VWR, United Kingdom). Thereafter, plasma was collected and stored at -20°C until further analysis.

Urine samples were obtained by placing the rats for 24h in a metabolic cage. Urine collections were centrifuged at 1500 rpm for 5 minutes (Centrifuge 5804R, Eppendorf, Belgium) to remove food particles and supernatants were stored at -20°C until further analysis.

2.6 Standard clinical tests

Standard clinical tests of plasma and urine samples were performed in the clinical laboratory of the hospital Ziekenhuis Oost-Limburg (ZOL) in Genk by using an automated analyzer (Cobas 8000 modular analyzer with P 800 and ISE 900 modules, Roche/Hitachi, Mannheim, Germany). In plasma samples, bilirubin, creatinine kinase (CK), creatinine (Jaffe's reaction), cys C, sodium and chloride were measured to investigate heart, kidney and liver damage (Table 4). On the other hand, the following clinical parameters were measured in urine samples as an indication for kidney function: creatinine (Jaffe's reaction), total protein, chloride and sodium. Based on the levels of creatinine in plasma and urine (24 hours collection), creatinine clearance was calculated via the formula: [$urine_{creatinine}$ (mg/dl) x $urine_{volume}$ (ml)]/[$plasma_{creatinine}$ (mg/dl) x 1440 (min) x bodyweight (kg)]. Additionally, the percentage fractional sodium excretion (FENa) was calculated as follows: 100 x [($urine_{sodium}$ (mmol/l) x $plasma_{creatinine}$ (mg/dl)]/[$plasma_{sodium}$ (mmol/l) x $urine_{creatinine}$ (mg/dl)]).

Table 4: Overview of the clinical parameters measured in urine and plasma samples.

	Heart	Kidney	Liver
Urinary parameters	/	Creatinine	/
		Total protein	
		Chloride	
		Sodium	
Plasma parameters	CK	Creatinine	Bilirubin
		Cys C	
		Chloride	
		Sodium	

Heart, kidneys and liver function are assessed via measuring different clinical parameters in plasma and urine samples. CK, creatinine kinase; Cys C, cystatin C.

2.7 Hemodynamic measurements

Rats were anesthetized with 2 - 4% isoflurane as previously explained. Incisions were made in the right side of the neck and left groin in order to reach the VCI via the vena jugularis dextra (Figure 2) and vena femoralis sinistra, respectively. Additionally, the LV pressure (LVP) was measured in the LV via the arteria carotis dextra. The blood vessels were isolated and dissected free from the surrounding tissues. Subsequently, the blood vessel was held under tension with forceps in order to facilitate puncture with a 24G needle. Before insertion, the catheter (SPR-320, Millar Instruments, AD Instruments, Germany) was calibrated to 0 mmHg in water of 37°C. Measurements were performed with LabChart 7 software (ADinstruments, Germany) and were continued for approximately five minutes to obtain stable measurements above and below the constriction. When all measurements were performed, heparin (1,000 I.U., LEO Pharma, Belgium) and an overdose of Nembutal (60 mg/ml, Ceva, Belgium) were injected intraperitoneally. The measurements in the VCI via the vena jugularis and vena femoralis provided CVP above and below the constriction, from which also the difference of these two was calculated. Arteria carotis measurements revealed systolic LVP and LV contractility/relaxation via dP/dt max/min. It should be noted that in contrary to the measurements above and below the constriction, the measurements via the arteria carotis were not completed in all rats (sham n = 5, VCI n = 3) due to practical limitations.

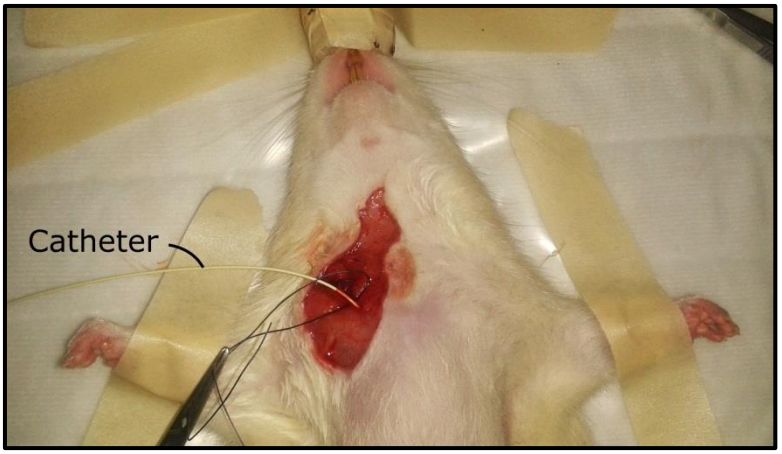

Figure 2: Hemodynamic measurement with catheter inserted via the vena jugularis dextra. The rat is anesthetized via a mouth mask (2 – 4% isoflurane) and is kept on a heating pad during the entire procedure. Paws are secured with tape in order to avoid movement.

2.8 Organ retrieval and histological analysis

After sacrifice, organs were retrieved from the rats in order to determine the weight of the heart, left ventricle, lungs, liver, kidneys, digestive system (stomach, spleen and small and large intestine) and spleen. Organ weight was normalized to tibia length. The heart was perfused with a Tyrode NT buffer (137 mM NaCl; 5,4 mM KCl; 0,5 mM $MgCl_2$; 1 mM $CaCl_2$; 11,8mM (Na)HEPES (Sigma-Aldrich, Belgium); and pH between 7,35 and 7,40) and a 540 mM KCl solution in order to preserve cardiomyocytes in a diastolic state. The heart, kidneys and liver were cut in transverse slices of 5 mm and were preserved in 4% paraformaldehyde (PFA) for 24h at 4°C. Next, 4% PFA was replaced by 70% ethanol in which tissues were preserved at 4°C until paraffination. Tissue sections of 5 - 6 µm were made with a microtome (Leica, Leitz 1512, Germany) and were stained with hematoxylin and eosin (H&E) to study tissue morphology and with Masson's trichrome or Sirius Red/Fast Green to evaluate fibrosis.

2.8.1 Hematoxylin and eosin staining

Paraffin sections were deparaffined and rehydrated in 100% xylene and an ethanol gradient from 100% to 70%. Additionally, sections were washed in distilled water and 1x phosphate buffered saline (PBS) before staining in hematoxylin. After a wash step in flowing tab water, sections were stained with eosin. Dehydration was performed by placing the sections in graded ethanol bathes from 70% to 100% and in 100% xylene. Finally, coverslips were mounted on the microscope slides with distyrene plasticizer xylene (DPX) mounting medium (Leica, Belgium). Tissue section were imaged by scanning with a Mirax Desk via Mirax scan and viewer software (Zeiss, Germany). Cardiac tissue was analyzed for myocardial wall thickness and renal tissue was analyzed for the width of Bowman's space with Pannoramic Viewer software 1.15.4 (3DHISTECH, Hungary). Mean cardiac wall thickness is determined by measuring eight randomly selected regions of the cardiac wall (as indicated in Figure 3A). In renal tissues, the mean width of bowman's space was calculated of ten glomeruli in which the width of Bowman's space was determined by measuring five randomly selected regions (as demonstrated for one glomerulus in Figure 3B). On the other hand, liver tissue was investigated for hepatocyte hypertrophy via analysis with AxioVision Rel. 4.6 software (Zeiss, Germany). Four randomly selected pictures at a 20x magnification were analyzed for nuclear and total cell surface (Figure 3C-E). The mean percentage hypertrophy for each tissue section was calculated with the percentage hypertrophy for each picture; ($area_{nucleus}/area_{total\ cell}$) x 100.

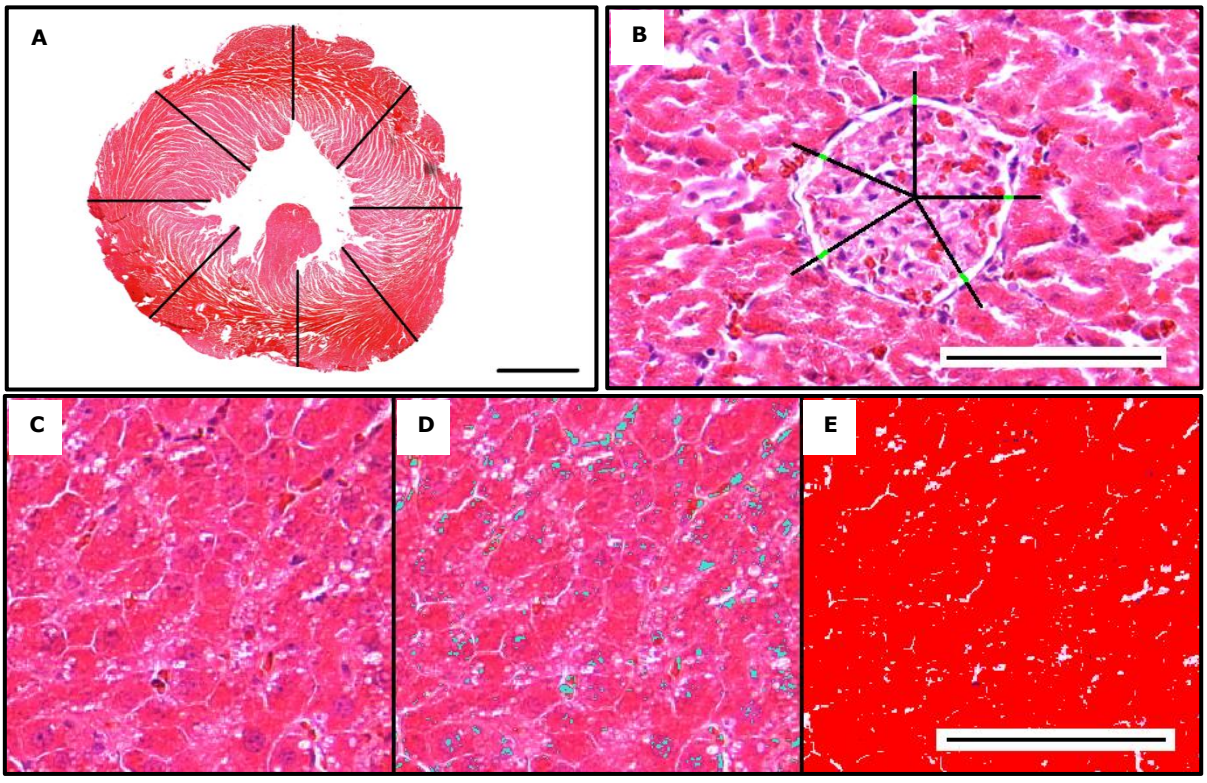

Figure 3: Examples of analysis performed to evaluate cardiac wall thickness **(A)**, width of Bowman's space (green) **(B)** and hepatocyte hypertrophy after H&E staining on paraffin-embedded tissues **(C-E)**. Comparison of original picture at a 20x magnification **(C)**, nuclei represented by a blue surface **(D)** and total cell area by a red surface **(E)** via AxioVision Rel. 4.6 software. Scale bar = 2000 µm **(A)**, 100 µm **(B-E)**.

2.8.2 Masson's trichrome staining

Paraffin sections were deparaffined and rehydrated as previously described, but only washed in MilliQ. Thereafter, staining was initiated by placing the tissue sections in hematoxylin mayer

solution followed by a wash step in flowing tab water. Next, the following bathes were included: Ponceau/Fuchsine staining, 1% phosphomolybdeen acid, aniline blue staining, phosphomolybdeen acid and 1% acetic acid. After every step, a wash step in MilliQ was included. Finally, the tissue sections were rehydrated, mounted and imaged as previously described. Fibrosis analysis was performed with the aid of AxioVision Rel. 4.6 software by quantifying the amount of red and blue colored tissue pixels in four random pictures at a 20x magnification for every tissue section. Mean percentage of fibrosis for each tissue section was determined by calculating the percentage fibrosis for every picture; ($area_{blue}$ / ($area_{red}$ + $area_{blue}$)) x 100. The red area is total cell surface, while blue represents connective tissue as a measure of fibrosis (Figure 4A-C).

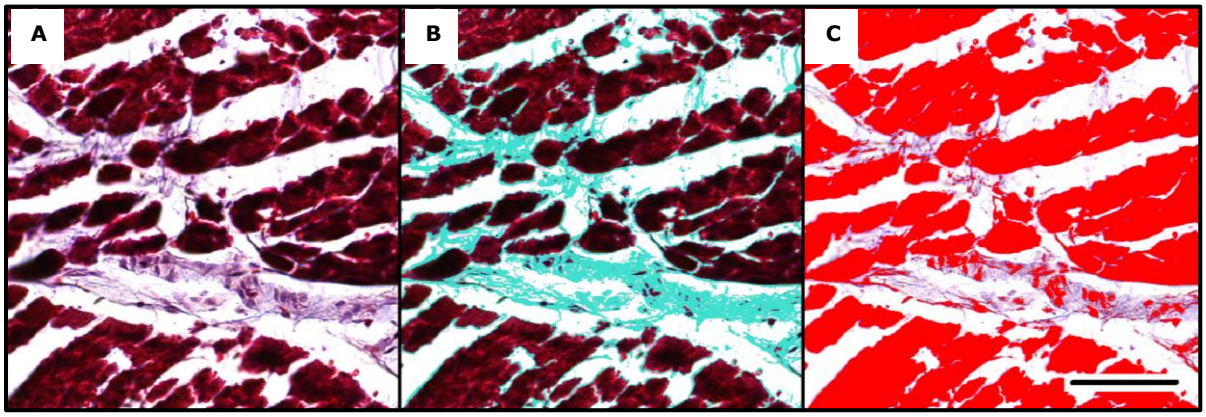

Figure 4: Example of analysis performed to measure the percentage fibrosis in paraffin-embedded tissue sections after Masson's trichrome staining. Comparison of original picture at a 20x magnification **(A)**, fibrotic tissue represented by a blue surface **(B)** and total cell area by a red surface **(C)** via AxioVision Rel. 4.6 software. Scale bar = 100 µm **(A-C)**.

2.9 Statistical analysis

All data are presented as mean ± SEM and analyzed with GraphPad Prism software (version 5.01, GraphPad software, USA). Normal distribution of data was tested with the Kolmogorov-Smirnov test. Statistical analyses were performed with an unpaired t-test or two-way repeated measures (RM) ANOVA test when data passed the normality test but were unpaired and paired, respectively. In case of paired not normally distributed data, a Mann-Whitney test was performed for every time-point as for unpaired data. Correlation analysis between variables was achieved via a Pearson test.

3 Results

3.1 Echocardiography

To assess cardiac morphology and functioning, echocardiographic analysis were performed at baseline and week 6 and 12 after sham-operation or VCI-constriction. No statistically significant changes in echocardiographic parameters were demonstrated in VCI-constricted rats (n = 7) compared to sham-operated rats (n = 6) after twelve weeks (Table 5).

Table 5: Echocardiographic parameters at baseline (week 0) and twelve weeks after sham operation or VCI constriction.

Parameter	Week	Sham (n = 6)	VCI (n = 7)
LVEDD (mm)	0	4.7 ± 0.2	5.3 ± 0.1
	12	7.3 ± 0.5	7.9 ± 0.4 *
LVESD (mm)	0	2.7 ± 0.2	2.9 ± 0.1
	12	4.1 ± 0.5	5.1 ± 0.2
PWT (mm)	0	0.85 ± 0.07	0.78 ± 0.05
	12	0.80 ± 0.05	0.78 ± 0.04
AWT (mm)	0	1.20 ± 0.06	1.17 ± 0.07
	12	1.04 ± 0.05	1.04 ± 0.06
HR (bpm)	0	396 ± 6	400 ± 12 *
	12	367 ± 14	361 ±22
EDV (µl)	0	111 ± 10	140 ± 6
	12	409 ± 52	460 ± 56
ESV (µl)	0	25 ± 4	30 ± 3
	12	98 ± 24	132± 15
SV (µl)	0	86 ± 11	110 ± 8
	12	311 ± 36	329 ± 45
CO (ml/min)	0	34 ± 5	44 ± 3
	12	113 ± 13	116 ± 16
EF (%)	0	76 ± 5	78 ± 3
	12	78 ± 4	78 ± 3
FS (%)	0	30 ± 4	31 ± 3
	12	30 ± 4	29 ± 2

Echocardiographic parameters compared between sham-operated (n = 6) and VCI-constricted (n = 7) rats. LVEDD, left ventricle end-diastolic diameter; LVESD, left ventricle end-systolic diameter; PWT, posterior wall thickness; AWT, anterior wall thickness; HR, heart rate; EDV, end-diastolic volume; ESV, end-systolic volume; SV, stroke volume; CO, cardiac output; EF, ejection fraction; FS, fractional shortening. Data are presented as mean ± SEM. * $p < 0.05$ between week 0 and 12 (Mann-whitney or unpaired t-test).

3.2 Standard clinical parameters

Different clinical parameters were investigated in urine and plasma samples obtained every three weeks during the follow-up period of twelve weeks. In the urine samples, only parameters of kidney function were measured. On the other hand, parameters of heart, kidney and liver function were assessed in plasma samples.

3.2.1 Heart function

To investigate cardiac injury, CK levels were measured in plasma samples. No statistically significant changes in CK levels were demonstrated in VCI-constricted rats (n = 7) compared to sham-operated rats (n = 6) (Figure 5). The pilot study demonstrated similar results (data not shown).

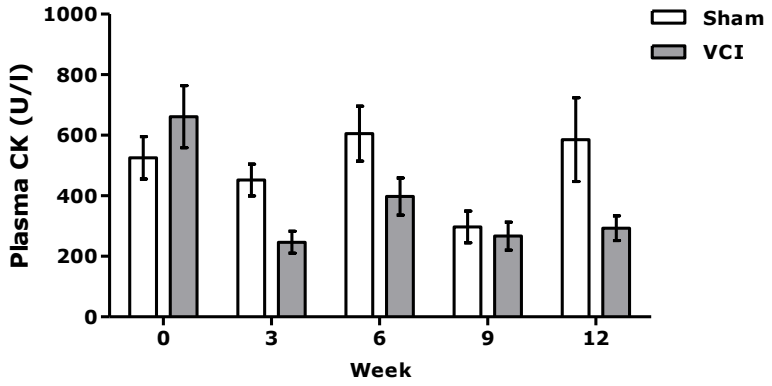

Figure 5: Creatine kinase (CK) levels in plasma samples compared between sham-operated (n = 6) and VCI-constricted (n = 7) rats. Data are presented as mean ± SEM. * $p < 0.05$ (two way RM ANOVA).

3.2.2 Kidney function

In urine and blood samples, different clinical parameters were measured in order to investigate different aspects of kidney function. Glomerular filtration rate was determined via creatinine clearance and assessed via plasma cys C levels. Electrolyte handling was investigated by measuring chloride and sodium levels in urine and plasma samples. Fractional sodium excretion was also calculated. Last, urinary total protein was measured to investigate glomerular damage.

3.2.2.1 Glomerular filtration rate

Urinary and plasma creatinine levels were measured to investigate and calculate creatinine clearance. No statistically significant changes were detected in urinary creatinine levels between sham-operated (n = 6) and VCI-constricted (n = 7) rats (Figure 6A). On the other hand, creatinine levels in plasma samples of VCI-constricted rats were significantly increased in week 9 and 12 (Figure 6B). Glomerular filtration rate was based on creatinine clearance and calculated via plasma and urinary creatinine levels of an 24 hours urine output; GFR = [$urine_{creatinine}$ (mg/dl) x $urine_{volume}$ (ml)]/[$plasma_{creatinine}$ (mg/dl) x 1440 (min)]. However, creatinine clearance showed no significant change after VCI constriction (Figure 7). On the other hand, plasma cys C was significantly increased in week 9 and 12 after VCI constriction (Figure 8). The pilot study showed similar results (data not shown).

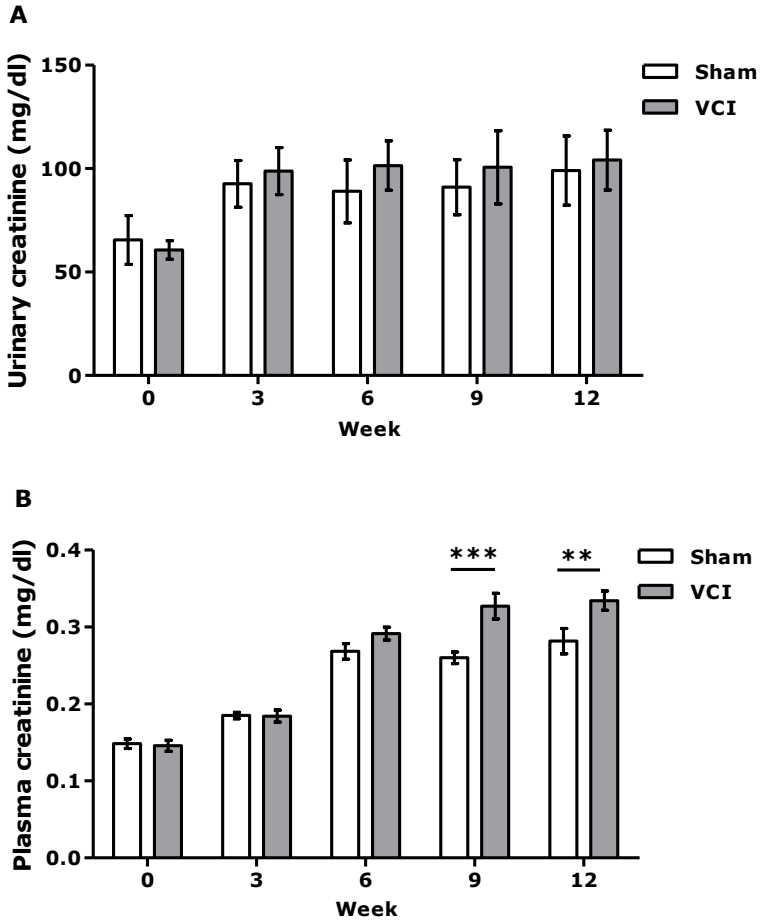

Figure 6: Urinary **(A)** and plasma **(B)** creatinine levels compared between sham-operated (n = 6) and VCI-constricted (n = 7) rats. Data are presented as mean ± SEM. * $p < 0.01$; *** $p < 0.001$ (unpaired t-test **(A)**; two way RM ANOVA **(B)**).

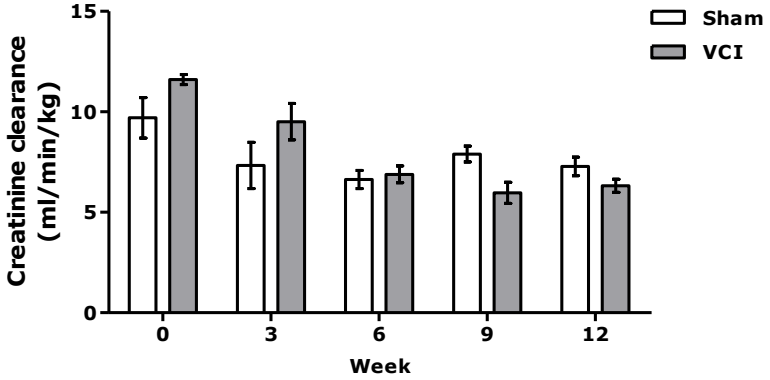

Figure 7: Creatinine clearance of sham-operated (n = 6) and VCI-constricted (n = 7) rats was calculated as follows: GFR = [$urine_{creatinine}$ (mg/dl) x $urine_{volume}$ (ml)]/[$plasma_{creatinine}$ (mg/dl) x 1440 (min)] (two way RM ANOVA). Data are presented as mean ± SEM.

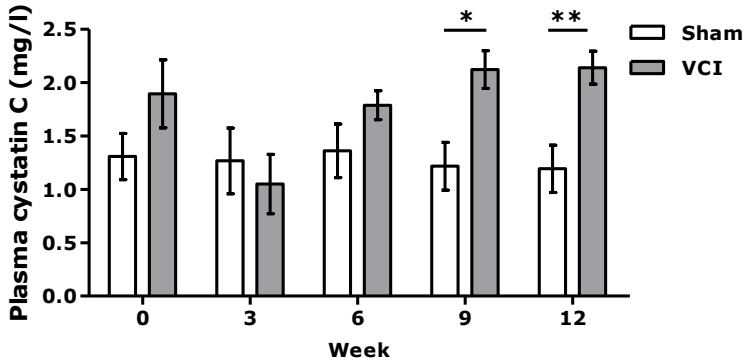

Figure 8: Plasma cystatin C levels of sham-operated (n = 6) and VCI-constricted (n = 7) rats. Data are presented as mean ± SEM. * $p < 0.05$; ** $p < 0.01$ (two way RM ANOVA).

3.2.2.2 Electrolyte handling

Chloride and sodium handling of the kidney was investigated by measuring urine and plasma levels of these electrolytes. Urinary electrolyte levels were normalized to urinary creatinine levels. No significant changes in urinary chloride (Figure 9A) and sodium (Figure 9B) were detected after VCI constriction. On the other hand, plasma chloride (Figure 10A) and sodium (Figure 10B) levels were significantly increased in VCI-constricted rats (n = 7) compared to sham-operated rats (n = 6) in week 9 and 12. Last, FENa was calculated via FENa% = 100 x ([$urine_{sodium}$ (mmol/l) x $plasma_{creatinine}$ (mg/dl)]/[$plasma_{sodium}$ (mmol/l) x $urine_{creatinine}$ (mg/dl)]). However, FENa was not significantly changed after VCI constriction (Figure 11). Similar results were obtained in the pilot study (data not shown).

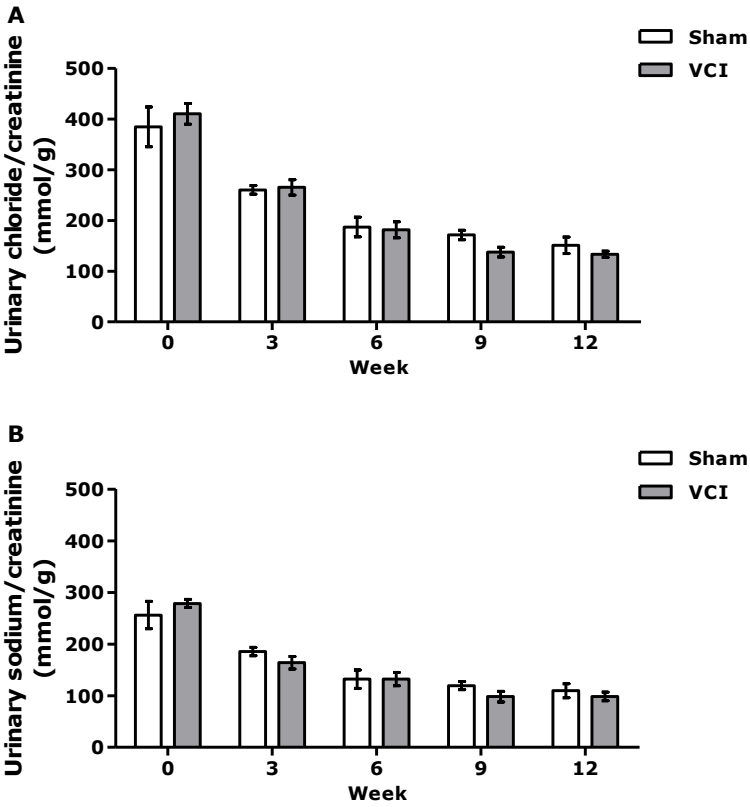

Figure 9: Urinary chloride **(A)** and sodium **(B)** levels compared between sham-operated (n = 6) and VCI-constricted (n = 7) rats. Urinary chloride and sodium levels are normalized to urinary creatinine levels. Data are presented as mean ± SEM. * $p < 0.05$; *** $p < 0.001$ (two way RM ANOVA).

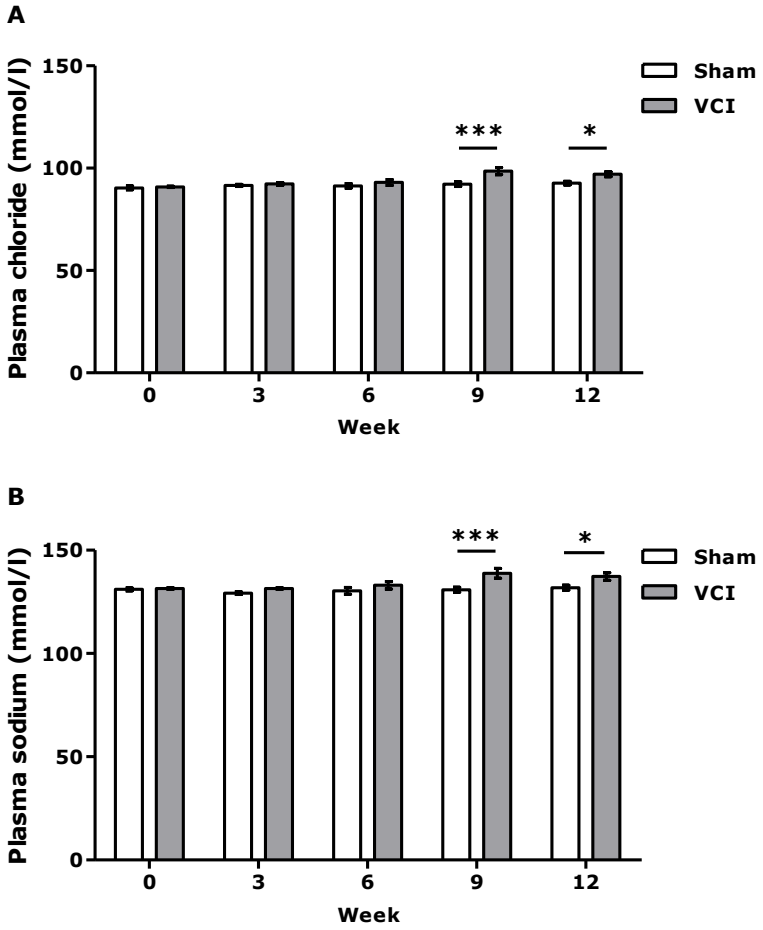

Figure 10: Plasma chloride **(A)** and sodium **(B)** levels compared between sham-operated (n = 6) and VCI-constricted (n = 7) rats. Data are presented as mean ± SEM. * $p < 0.05$; *** $p < 0.001$ (two way RM ANOVA).

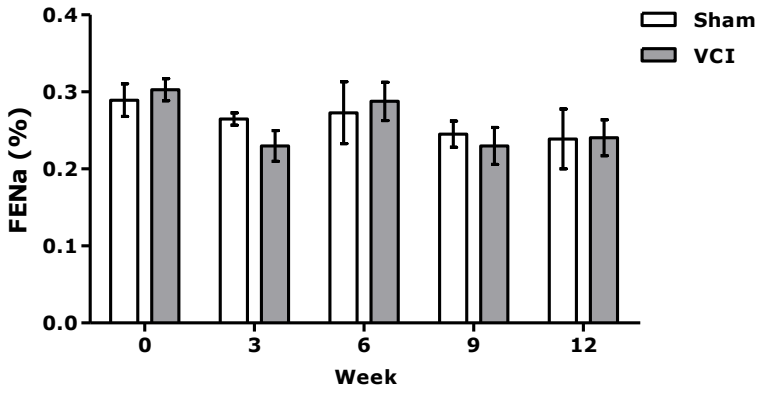

Figure 11: Fractional sodium excretion (FENa) of sham-operated (n = 6) and VCI-constricted (n = 7) rats. Fractional sodium excretion was calculated via the following formula: FENa% = 100 x ([$urine_{sodium}$ (mmol/l) x $plasma_{creatinine}$ (mg/dl)]/[$plasma_{sodium}$ (mmol/l) x $urine_{creatinine}$ (mg/dl)]). Data are presented as mean ± SEM.

3.2.2.3 Glomerular damage

Urinary total protein levels were measured as a marker of glomerular damage. No statistically significant changes were detected in urinary total protein levels normalized to creatinine levels between sham-operated (n = 6) and VCI-constricted (n = 7) rats (Figure 12). Similar results were observed in the pilot study (data not shown).

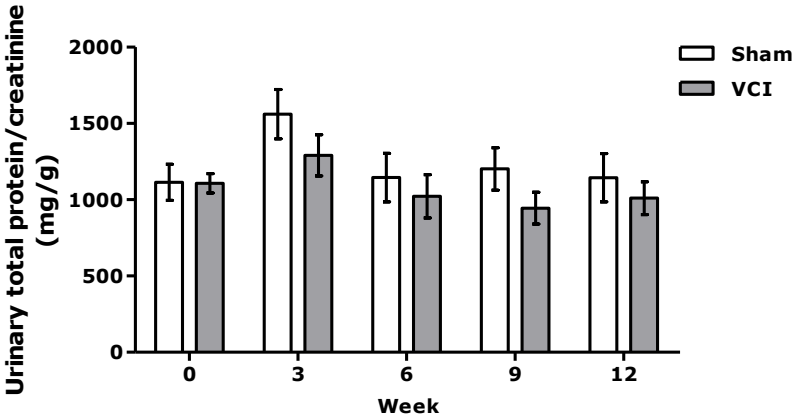

Figure 12: Urinary total protein levels compared between sham-operated (n = 6) and VCI-constricted (n = 7) rats (unpaired t-test). Urinary total protein is normalized to urinary creatinine levels. Data are presented as mean ± SEM.

3.2.3 Liver function

To investigate the influence of VCI constriction on liver function, plasma bilirubin levels were compared between sham-operated (n = 6) and VCI-constricted (n = 7) rats. The bilirubin levels were increased significantly by VCI constriction in week 6, 9 and 12 (Figure 13). Similar results were demonstrated in the pilot study, although not statistically significant (data not shown).

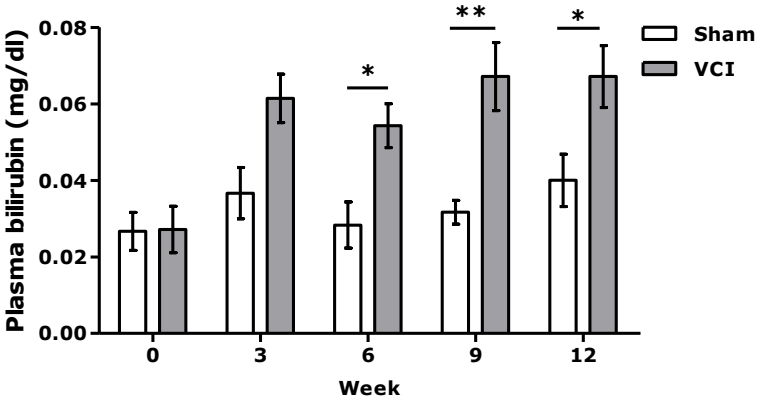

Figure 13: Plasma bilirubin in sham-operated (n = 6) and VCI-constricted (n = 7) rats. Data are presented as mean ± SEM. * $p < 0.05$; ** $p < 0.01$ (two way RM ANOVA).

3.3 Hemodynamic measurements in the vena cava inferior and left ventricle

Hemodynamic measurements were performed at the end of the follow-up period in week 12. The CVP was measured in the VCI above the constriction via the vena jugularis dextra and below the constriction via the vena femoralis sinistra. The CVP measured via the vena jugularis was not influenced by VCI constriction, while the CVP measured via the vena femoralis was significantly increased compared between sham-operated (n = 6) and VCI-constricted rats (n = 7) (Figure 14A). The difference between the CVP measured above and below the constriction was calculated by subtracting the CVP measured via the vena jugularis from the CVP measured via the vena femoralis. This difference was significantly higher in VCI-constricted rats (Figure 14B). The pilot study provided similar results, although not statistically significant (data not shown).

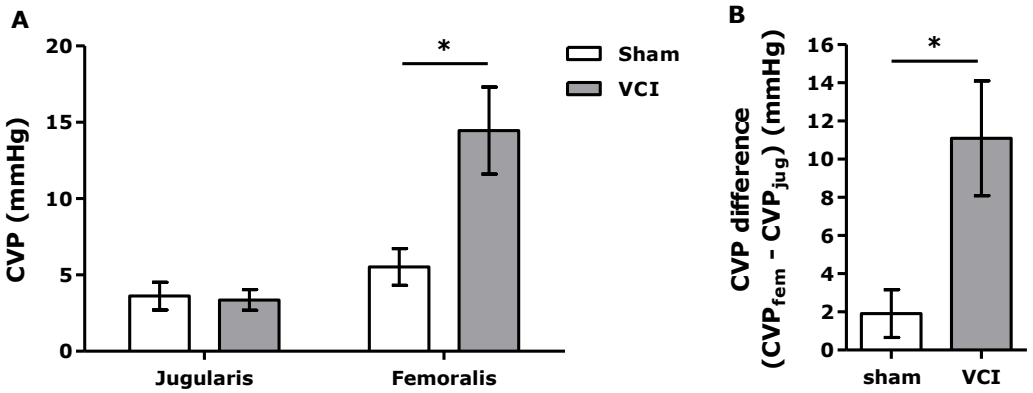

Figure 14: Central venous pressure (CVP, mmHg) in the VCI reached via the vena femoralis and vena jugularis **(A)** of sham-operated (n = 6) and VCI-ligated (n = 7) rats. The difference between the CVP above and below the constriction measured via the vena femoralis and vena jugularis (CVP_{fem} – CVP_{jug}) **(B)** in sham-operated and VCI-ligated rats. Data are presented as mean ± SEM. * $p < 0.05$ (unpaired t-test).

Additionally, the LVP at systole was measured and the dP/dt max and min were calculated in the LV. No statistically significant changes was demonstrated in LVP and dP/dt max and min between sham-operated and VCI-ligated rats (Table 6).

Table 6: Hemodynamic measurements in left ventricle.

Measurement	Sham (n = 5)	VCI (n = 3)
LVP (mmHg)	105.7 ± 6.6	118.5 ± 10.4
dP/dt max (mmHg/s)	5311.4 ± 405.0	7041.2 ± 1145.4
dP/dt min (mmHg/s)	-4391.9 ± 347.4	-5246.5 ± 920.4

Left ventricular pressure (LVP) and dP/dt max and min compared between sham-operated (n = 5) and VCI-constricted (n = 3) rats. Data are presented as mean ± SEM.

3.4 Physical parameters

Bodyweight was evaluated every week during the twelve week follow-up period. No statistically significant difference was shown in bodyweight between sham-operated (n = 6) and VCI-constricted (n = 7) rats (Figure 15). When rats were sacrificed, organs were retrieved in order to investigate differences in organ weight between sham-operated and VCI-constricted rats. Organ weight was normalized to tibia length. Heart, left ventricle, lungs, kidneys, digestive system and liver weight showed no statistically significant differences in VCI-constricted rats compared to sham-operated rats. However, the spleen showed a significant increase in weight after VCI constriction (Table 7). These results confirm the data regarding the physical parameters of the pilot study (data not shown).

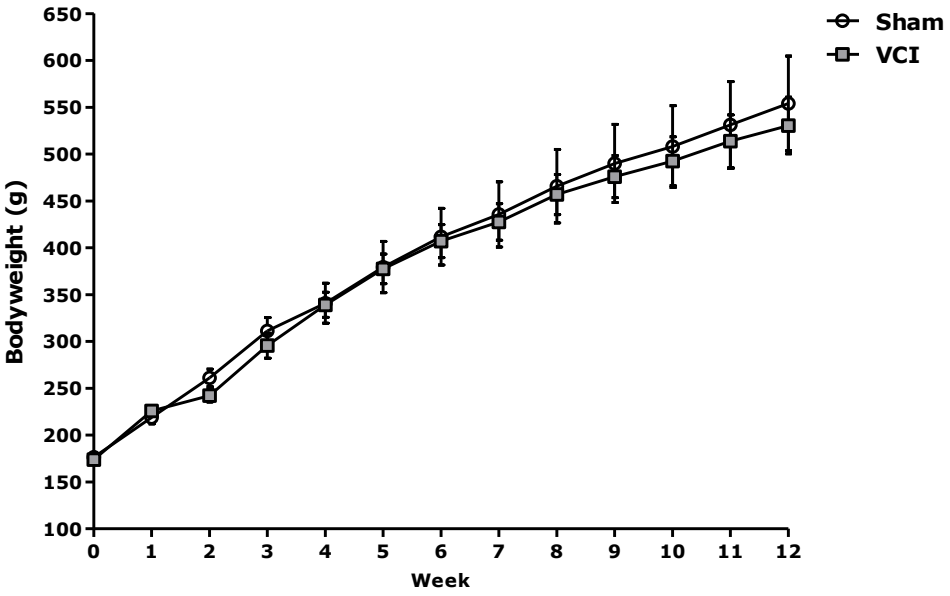

Figure 15: Bodyweight at weekly intervals during the twelve-week follow-up of sham-operated (n = 6) and VCI-constricted (n = 7) rats (two-way RM ANOVA). Data are presented as mean ± SEM.

Table 7: Organ weight normalized to tibia length (mg/mm).

Organ weight/tibia length (mg/mm)	Sham (n = 6)	VCI (n = 7)
Heart weight/tibia length (mg/mm)	39.3 ± 1.2	42.9 ± 3.3
Left ventricle weight/tibia length (mg/mm)	21.7 ± 1.1	23.4 ± 1.2
Kidneys weight/tibia length (mg/mm)	40.1 ± 1.7	39.7 ± 3.7
Lung weight/tibia length (mg/mm)	74.1 ± 6.1	75.7 ± 4.0
Digestive system weight/tibia length (mg/mm)	813.0 ± 79.6	807.3 ± 37.1
Spleen weight/tibia length (mg/mm)	19.8 ± 1.0	26.6 ± 1.4**
Liver weight/tibia length (mg/mm)	419.3 ± 47.0	497.6 ± 34.1

The weight of the heart, left ventricle, kidneys, lungs, digestive system, spleen and liver compared between sham-operated (n = 6) and VCI-constricted rats (n = 7). Data are presented as mean ± SEM. ** $p < 0.01$ (unpaired t-test).

3.5 Morphological parameters

Heart, kidney and liver tissue sections were evaluated on morphological changes via a H&E staining. These tissue sections were analyzed for myocardial wall thickness, the width of Bowman's space and hepatocyte hypertrophy, respectively. No statistically significant difference between sham-operated (n = 6) and VCI-constricted (n = 7) rats was demonstrated in cardiac wall thickness (Figure 16A-C) and hepatocyte hypertrophy (Figure 16G-I). On the other hand, there was a statistically significant increase in the width of Bowman's space after VCI constriction (Figure 16D-F). Similar results were obtained in the pilot study, although no statistically significant difference was observed in the width of Bowman's space (data not shown).

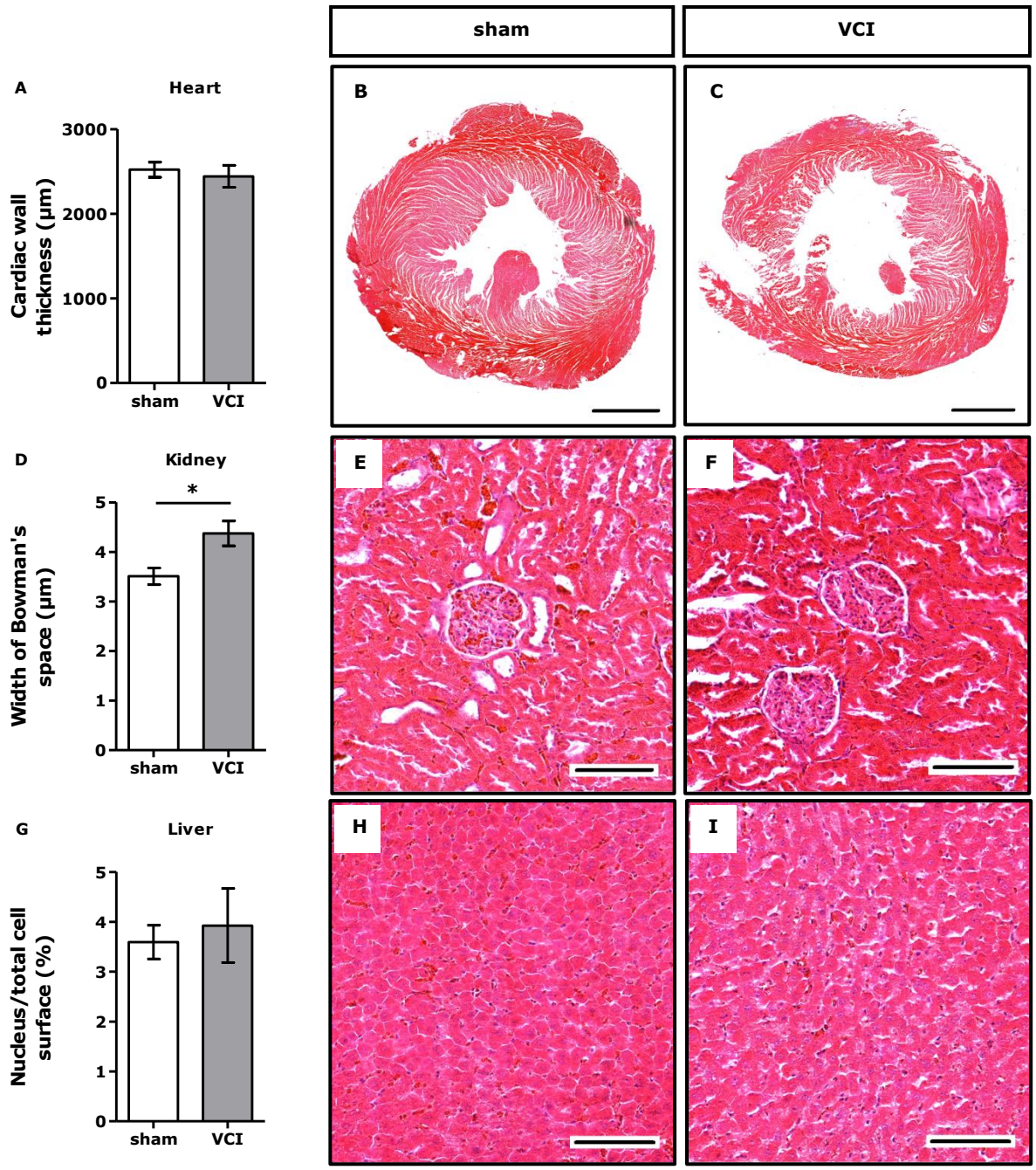

Figure 16: H&E staining of paraffin-embedded heart, kidney and liver tissue sections. Morphological parameters (cardiac wall thickness **(A-C)**, width of bowman's space **(D-F)** and hepatocyte hypertrophy **(G-I)**, respectively) compared between sham-operated (n = 6) and VCI-constricted (n = 7) rats. Data presented as mean ± SEM. Scale bar = 2000 µm **(B-C)**, 100 µm **(E-F, H-I)**. * $p < 0.05$ (unpaired t-test).

3.6 Fibrosis

Masson's trichrome staining of heart, kidney and liver tissue was used to investigate the percentage of fibrosis present in these tissue sections. There were no statistically significant changes found in the percentage fibrosis of heart (Figure 17A-C) and kidney (Figure 17D-F) tissues, however, the percentage fibrosis in the liver (Figure 17G-I) was statistically significant higher in the VCI-constricted rats (n = 7) compared to sham-operated (n = 6) rats.

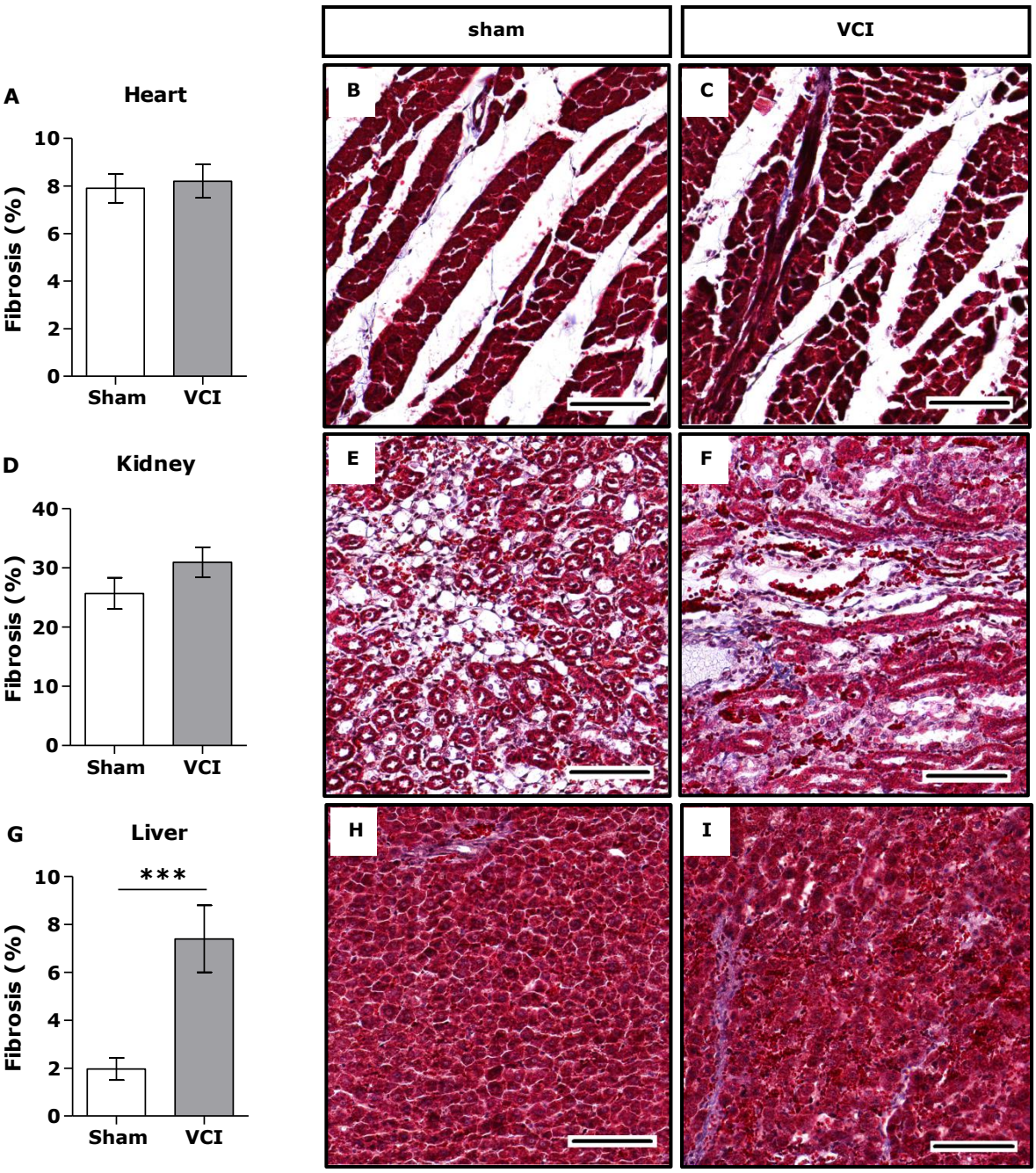

Figure 17: Masson's trichrome staining of paraffin-embedded heart **(A-C)**, kidney **(D-F)** and liver **(G-I)** tissue sections compared between sham-operated (n = 6) and VCI-constricted (n = 7) rats. Data are presented as mean ± SEM. Scale bar = 100 µm **(B, C, E, F, H, I)**. *** $p < 0.001$ (unpaired t-test).

Both the liver function test based on plasma bilirubin levels and the percentage hepatic fibrosis showed significant liver damage in the VCI-constricted rats. Therefore, a correlation analysis was performed and a positive correlation was demonstrated between these two variables ($R^2 = 0.6$; $p = 0.002$) (Figure 18).

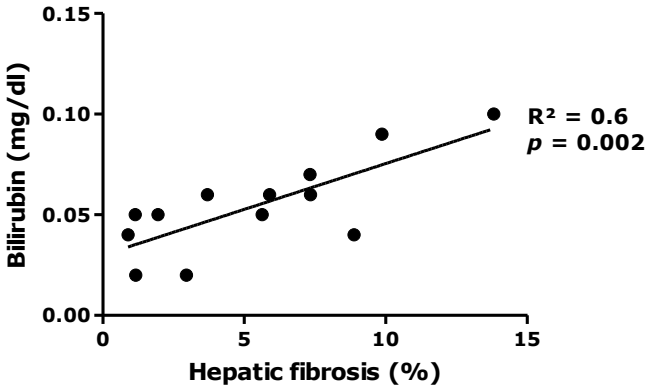

Figure 18: Correlation between the percentage hepatic fibrosis and plasma bilirubin levels. $R^2 = 0.6$; $p = 0.002$ (Pearson).

4 Discussion and outlook

The presented results provide the basis for the validation of the rat model for abdominal venous congestion. These also indicate how heart, kidney and liver function are influenced by VCI constriction. Moreover, it is possible to indicate which organ is targeted first.

4.1 Pressure in the vena cava inferior and left ventricle

The CVP measured in the VCI via the vena femoralis (i.e. below the constriction) was increased in VCI-constricted rats. This was expected as VCI constriction causes an accumulation of blood below the constriction, leading to an increase in abdominal CVP. Consequently, a decrease in CVP measured via the vena jugularis was predicted since blood is blocked below the constriction, which lowers blood flow in the VCI above the constriction. However, this decrease in CVP measured via the vena jugularis was not confirmed in the presented project. This could be explained by the activation of compensatory mechanisms that mask a decrease in CVP above the constriction. Activation of the RAAS and SNS could have led to vasoconstriction of the VCI and fluid retention to increase CVP to normal values. Meier *et al*. (2006) measured a CVP via the vena jugularis of 3 mmHg in healthy male Sprague-Dawley rats, which corresponds with the data of the presented study (Figure 14A) (58). On the other hand, the presented project showed an increase in CVP below the constriction to 14.5 mmHg, which is in accordance with results of Paganelli *et al*. (1988) investigating VCI constriction in dogs. The exact location of VCI constriction was not specified in this study but the duration of VCI constriction was acute (hours to days), which is in contrast with the chronic constriction (12 weeks) induced during the presented project. Still, this study showed an increase in CVP below the constriction from 3 mmHg to 14 mmHg, which corresponds with the elevated CVP from 4 mmHg to 14.5 mmHg in the presented study (59). It should be noted that this study was performed in dogs, but to our knowledge no similar data are available in rats.

As absolute values can mask changes in CVP due to inter-individual variation between the rats, the difference between the CVP above and below the constriction was calculated. This difference was significantly higher in VCI-constricted rats, which confirms the increase in abdominal CVP due to VCI constriction (Figure 14B). To conclude, these data give a first validation on the development of abdominal venous congestion after VCI constriction. Additionally, a CVP of 15 mmHg was also demonstrated in acute decompensated HF patients and CVP increased further with increasing IAP (11). This underlines the positive correlation between CVP and IAP, but also the biological relevance of the increase in abdominal CVP achieved in this rat model compared to the increased CVP in HF patients.

Additionally, the systolic LVP and LV dP/dt max and min measured via the arteria carotis dextra were unchanged after VCI constriction, although an increase in all measurements could be suggested after VCI constriction (Table 6). In this rat model of abdominal venous congestion, it is expected that (neuro)humoral systems are activated due to VCI constriction (as described in 1.2.2), which results in increased myocardial contraction and relaxation to maintain CO (60). The increase in contraction potential as part of the systolic phase was reflected in the increased systolic LVP. The measures of sham-operated rats correspond with results of other studies investigating cardiac function in male Sprague-Dawley rats. For example, systolic LVP was 100 mmHg and dP/dt

max and min were between 4500-5000 mmHg/s for control rats in a study of Huang *et al*. (2007), who investigated a new therapeutic strategy to improve cardiac function in diabetic rats (61). Huang *et al*. (2007) also showed that these measures decrease in the failing heart. Taken together, this may indicate that the presented project showed the first effects of VCI constriction on heart function by increasing contraction and relaxation, rather than chronic effects associated with deteriorating heart function. Still, these effects were statistically not significant between sham-operated and VCI-constricted rats. This could be explained by the limited number of animals in which these measurements could be performed (sham n = 5, VCI n = 3), but still provides a first rationale that the follow-up period was too limited in order to impair heart function.

4.2 Congestion in the abdomen and organs

Bodyweight was monitored weekly during the follow-up period and VCI-constricted rats showed a lower increase in bodyweight after surgery compared to sham-operated rats but both groups showed an equal bodyweight by week 5 (Figure 15). No statistically significant difference in bodyweight was demonstrated between sham-operated and VCI-constricted rats. It was expected that bodyweight would increase after VCI constriction due to activation of (neuro)humoral pathways leading to increased fluid retention. Lala *et al*. (2015) showed via a post hoc analysis of the Diuretic Optimization Strategy Evaluation in Acute Decompensated Heart Failure (DOSE-AHF) and Cardiorenal Rescue Study in Acute Decompensated Heart Failure (CARRESS-HF) trials that patients hospitalized with acute HF and treated for congestion display a decrease in bodyweight after treatment. This decrease in bodyweight was also related to the severity of congestion but this pattern was not consistent and decongestion could not be predicted based on bodyweight. This showed that there could also be other factors contributing to bodyweight loss with decongestive therapy including inter-individual variation in the amount of fluid retention (62). Similarly, an increase in bodyweight after VCI constriction may be masked due to a variation between rats, which is demonstrated in the presented project. Moreover, the results suggest that VCI constricted rats had a lower average bodyweight by week 12. This may indicate that VCI constriction had an effect on overall health and appetite of these rats. Taken together, as there was no effect on bodyweight by VCI constriction, this suggests that VCI constriction did not lead to overt clinical signs (e.g. ascites) of abdominal congestion due to a fluid buildup in the abdomen. However, ascites is only demonstrated in a small number of patients with increased IAP in congestive HF (15). Therefore, bodyweight is not the most important determinant for the validation of this rat model for abdominal venous congestion.

On the other hand, an increase in organ weight was expected since abdominal congestion also influences other organs as described in 1.2.1.2. An increase in heart weight, however, is expected to be the consequence of myocardial hypertrophy. The presented project demonstrated no effect of VCI constriction on normalized weight of the heart, left ventricle, lungs, liver, kidneys and digestive system. Only spleen weight was increased in the VCI group (Table 7). This can be explained by the function of the spleen to store blood in its vasculature to avoid volume overload and misdistribution throughout the body, which leads to an increase in spleen weight due to fluid buildup (15, 23). To conclude, the increase in spleen weight gives an indication that abdominal venous congestion was being developed in VCI-constricted rats. These data together with the increase in abdominal CVP

validate the rat model of abdominal venous congestion. The increase in abdominal CVP validates the hemodynamic changes after VCI constriction, while the increased spleen weight confirms the effect of VCI constriction in the abdomen.

4.3 Echocardiography

Echocardiographic analysis were performed in order to follow-up cardiac function after VCI constriction. It was expected that hemodynamic changes induced via VCI constriction would activate compensatory mechanisms in the heart to maintain CO. However, no significant changes were observed in the echocardiographic parameters after twelve weeks of VCI constriction (Table 5). The follow-up period of twelve weeks may be insufficient to develop functional changes in the heart. This notion is supported by the results of the hemodynamic measurements in the LV, which showed an increase in contraction and relaxation after VCI constriction. It could be speculated that the increase in relaxation is reflected in a suggestive increased EDV after VCI constriction, which could be seen as a compensation to increase CO. However, ESV is also higher in the VCI group, indicating that absolute values can differ between both groups but that cardiac performance is maintained in both groups as CO is comparable. Nevertheless, the data obtained in the presented project are similar to the results presented by Watson *et al*. (2004), who investigated baseline echocardiographic values in male Sprague-Dawley rats (63). This shows the validity of the methods used to determine these echocardiographic parameters.

4.4 Effect of abdominal congestion on organ function

The effects of VCI constriction on heart, kidney and liver function were determined via standard clinical tests on urine and plasma samples. Liver function parameters were included as the pilot study showed a trend in increased liver weight normalized to tibia length, which was not confirmed by the presented project (data not shown).

It should be noted that plasma samples were hemolytic, which is the release of hemoglobin and other intracellular components from red blood cells into the plasma due to damage of the cell membrane. This is probably attributed to a turbid blood withdrawal via the tail vein of the rat. Different clinical parameters (i.e. sodium, chloride, total protein, bilirubin and CK) are influenced by hemolysis and results should be interpreted with caution (64). Therefore, baseline measurements are compared with data of other studies to confirm the results despite of hemolysis.

4.4.1 Heart function

Heart function was assessed by measuring plasma CK activity. It was expected that CK activity would increase after VCI constriction, since CK is released from the heart into the blood when the myocardium is damaged. However, the presented data suggest a decline of CK activity levels in VCI constricted rats compared to baseline measurements (Figure 5). Baseline CK values of 600 U/l are confirmed by Du *et al*. (2016) investigating myocardial ischemia-reperfusion injury in male Sprague-Dawley rats, but this study also showed an increase in CK activity after myocardial damage (65). This demonstrates that increased plasma CK activity levels are observed after acute cardiac injury, but VCI constriction did not cause an acute deteriorating condition of the heart.

The decreased CK activity can be explained by a reduced metabolic efficiency of cardiomyocytes as occurs in heart failure and cardiac remodeling due to phenotypic changes. Normal fatty acid oxidation involves creatine kinase, while less efficient ATP-producing pathways do not use CK, which results in lower CK activity (66). Another possible explanation for decreased CK activity after VCI constriction can be found in the relation between glutathione and CK. Gunst *et al*. (1998) showed that in case of organ failure CK activity levels should be assessed with caution since the loss of CK activity can be explained by a depletion of extracellular glutathione (67). This notion can be supported by the finding that glutathione levels are decreased in chronic heart failure patients as demonstrated by Radovanovic, *et al*. (2012) (68). Glutathione normally aids in the protection against ROS. Therefore, decreased CK activity may be explained by an increase in oxidative stress, which targets enzymes and proteins including CK (67). Taken together, other parameters should be tested to confirm to assumption that there is shift in energy metabolism of the heart or that glutathione levels could influence CK levels after VCI constriction.

It can be concluded that there was no direct cardiac damage caused by VCI constriction. This is not only suggested by decreased CK activity, but also by the results of the hemodynamic measurements in the LV and the echocardiographic analyses as these also did not show a significant decline in cardiac function by VCI constriction.

4.4.2 Kidney function

In urine and blood samples, different clinical parameters were measured in order to investigate different aspects of kidney function after VCI constriction. Glomerular filtration rate was determined via creatinine clearance and assessed via plasma cys C levels, while electrolyte levels (chloride and sodium) together with FENa were assessed to investigate salt retention. Finally, urinary total protein was measured as an indication for glomerular damage.

4.4.2.1 Glomerular filtration rate

Glomerular filtration rate based on creatinine clearance was expected to decrease after VCI constriction as explained in paragraph 1.2.1.1. In the presented project, there was a significant increase visible in plasma creatinine levels after VCI constriction (Figure 6A). However, no significant differences were found in urinary creatinine levels and creatinine clearance between sham-operated and VCI-constricted rats (Figure 6B, Figure 7). In a study of Ashtiyani *et al*. (2013) investigating renal reperfusion injury, a creatinine clearance of 6 ml/min/kg was observed in sham-operated male Sprague-Dawley rats, which is similar to the values of the presented study (69). This supports the reliability of the presented results despite hemolysis. It is speculated that creatinine clearance first increases and then declines after VCI constriction. This shift takes place around week 6 and a similar observation has been reported by Damman *et al*. (2009) in patients with cardiovascular diseases. This study showed that GFR gradually rises with increasing CVP until CVP increases above 6 mmHg after which GFR declines. The initial increase may be a reflection of hemodynamic changes leading to increased renal perfusion, while later the increased CVP results in backward failure and decreased renal perfusion (70). It is possible that these mechanisms also caused the shift in GFR after VCI constriction during the follow-up period of the presented study.

On the other hand, cys C levels showed a significant increase from week 9 in VCI-constricted rats (Figure 8). The increased plasma cys C levels could indicate a decrease in GFR although creatinine clearance was not significantly decreased. As shown by a meta-analysis of Dhamidharka *et al*. (2002), cys C is considered to be a better marker of GFR then creatinine clearance. This is evidenced by better correlation coefficients and greater receiver operating characteristic (ROC)-plot area under the curve (AUC) values (71). Additionally, creatinine has several limitations as an endogenous marker of GFR since plasma creatinine levels are influenced by body mass, gender, age, protein intake, inflammation and other routes of clearance can be addressed besides filtration (72). If cys C is considered to be a better marker of GFR, the presented data could indicate a reduction in GFR after VCI constriction. However, cys C values of the presented project are in contrast with a study of Efrati *et al*. (2011), who investigated AKI via unilateral nephrectomy in male Sprague-Dawley rats. Efrati *et al*. (2011) showed a cys C value in the sham group of 0.6 mg/l and of 1.1 mg/l after unilateral nephrectomy (73). The presented project showed a baseline value of 1.5 mg/l. This difference could be explained by the presence of hemolysis in blood samples, although other parameters were not influenced by hemolysis. It could also be that a difference in technique to measure cys C levels (ELISA vs. automatic analyzer) may influence the absolute levels of cys C due to a difference in sensitivity for cys C. Additionally, Efrati *et al*. (2011) obtained blood samples only 24-168 hours after surgery, while the presented project sampled blood every three weeks. Taken together, it is still valuable to compare cys C values between sham-operated and VCI-constricted rats. Therefore, it is concluded that GFR is decreased based on plasma cys C levels, but creatinine clearance only suggests a decrease in GFR.

4.4.2.2 Electrolyte handling

No statistically significant effect of VCI constriction on urinary electrolyte levels was demonstrated (Figure 9), but an increase in plasma chloride and sodium levels was observed in week 9 and 12 after surgery (Figure 10). The increase in plasma electrolyte levels was expected due to the activation of hemodynamic and (neuro)humoral mechanisms leading to salt retention (as described in 1.2.1 and 1.2.2). However, the presented data did not show a decrease in urinary electrolyte levels. Additionally, FENa was not significantly different between VCI constricted and sham-operated rats. This was also expected to decrease due to salt retention. As previously explained, the hemolytic factor of plasma samples could influence the results of electrolyte levels in the blood. However, when comparing baseline data of the presented project to control experimental rats in other studies investigating kidney injury in Sprague-Dawley rats, results are similar with blood sodium levels of 140 mmol/l, blood chloride levels of 100 mmol/l and FENa of 0.40% (74).

4.4.2.3 Glomerular damage

Urinary total protein level was measured to investigate glomerular damage, but no significant difference in total protein level normalized to urinary creatinine levels was observed after VCI constriction (Figure 12). It was expected that total protein in the urine would increase because of damage to the glomerular membrane, which is mostly seen in hypertensive nephropathies. First, Doty *et al*. (1999) showed that increased renal venous pressure leads to proteinuria in a swine model of renal vein constriction combined with unilateral nephrectomy (19). Similar, VCI constriction was expected to cause leakage of proteins to the urine due to increased

intraglomerular pressure. As renal vein constriction has a more direct effect on renal venous pressure then VCI constriction, VCI constriction may not be sufficient to increase the total protein level. Additionally, blood samples in the presented project were obtained three weeks after VCI constriction, while Doty *et al*. (1999) assessed total protein levels two hours after renal vein constriction. Second, it should be noted that urinary total protein normalized to urinary creatinine is a less accurate method to measure proteinuria, especially in the case of low relative molecular mass proteinuria. This could contribute to false lower total protein levels. By including specific microglobulins into the test panel, a specific classification of proteinuria can be made (75).

In conclusion, VCI constriction seems to have a limited effect on kidney function as creatinine, cys C, chloride and sodium levels were increased in the plasma, but no changes were detected in urinary creatinine, chloride and sodium levels, creatinine clearance and FENa. This could be explained by the enormous reserve capacity of the kidney. The kidney can maintain normal creatinine levels and GFR even when the kidney is damaged until 50% of nephrons are lost (76). This reserve capacity could mask the effects of VCI constriction on kidney function. Therefore, it could be that the follow-up period was too short in order to induce overt kidney damage.

4.4.3 Liver function

Bilirubin levels were measured to investigate liver function. Bilirubin is the end-product of heme breakdown and is transported to the liver bound to albumin. In the liver, it is removed from the plasma and is conjugated with glucuronic acid, which is excreted in via the bile (77). The presented data showed a significant increase in bilirubin levels from week 6 after VCI constriction (Figure 13). These results were expected as it was shown by Van Deursen *et al*. (2010) that in HF patients there is a correlation between elevated CVP and total bilirubin. Bilirubin levels are suggested to be increased due to reduced hepatic perfusion and congestion of the liver, which leads to hepatocyte necrosis resulting in impaired heme breakdown and accumulation of bilirubin in the plasma (78). In a study of Meier *et al*. (2006) investigating a new model of the abdominal compartment syndrome, bilirubin levels of control Sprague-Dawley rats were around 0.09 mg/dl (58). These control measurements are not in accordance with the results of the presented project as the bilirubin levels of sham-operated rats stay around 0.3 mg/dl during the follow-up period. This difference in results can be explained by the fact that Meier used female and male rats and sampled blood six hours after induction of the abdominal compartment syndrome. This is in contrast with the male rats and three-weekly blood sampling in the presented project. Still, it can be concluded that VCI constriction caused an increase in bilirubin level, which indicates a deterioration of liver function.

4.5 Morphological changes induced by abdominal venous congestion

Morphological changes in the heart, kidneys and liver were assessed to give a more complete understanding on the effects of abdominal venous congestion besides functional changes (Figure 16). First, in HF there are different compensatory mechanisms present to preserve CO. Changes in myocardial wall thickness is one of these mechanisms (79). After VCI constriction, cardiac wall thickness was expected to be increased as a consequence of myocardial hypertrophy to increase contractility. A cardiac wall thickness of 2500 µm is confirmed by Sunagawa *et al*. (2014), who observed LV cardiac wall thickness in rats with and without myocardial infarction. This study

showed a doubling of cardiac wall thickness in the non-infarcted area after induction of myocardial infarction (80). These overt changes were not observed in the presented project. This can be explained by the fact that VCI constriction also had no significant effect on LV contractility as demonstrated by the hemodynamic measurements in the LV. Additionally, the echocardiographic data supported the notion that cardiac function was not affected by VCI constriction. Therefore, no increase in cardiac wall thickness via hypertrophy was required as CO was maintained after VCI constriction.

Second, an increase in renal venous pressure causes an elevation in the hydrostatic pressure in Bowman's space (81). Consequently, it is expected that this would lead to enlargement of Bowman's space. Kotyk *et al*. (2015) measured the width of Bowman's space in Albino rats with chronic kidney disease. This study showed that in healthy rats the width of Bowman's space is 6 µm while in rats with chronic kidney disease this can double (82). The value of these healthy rats is in the same range as sham-operated rats of the presented project, indicating the accuracy of the method to measure the width of Bowman's space. The width of Bowman's space was significantly increased after VCI constriction, which indirectly suggests that renal venous pressure was elevated. This should lead to a decrease in GFR due to compression of the distal tubule by the surrounding venules (as described in 1.2.1.1). However, GFR was not statistically significant decreased in both parameters assessing GFR in the presented project (creatinine clearance and plasma cys C levels). Total protein levels also did not show any damage to the glomerular membrane, while an increase in the width of bowman's space suggests damage of the glomerulus. These inconsistencies could be explained by the high reserve capacity of the kidney before showing a deteriorating function, which could already be visible in kidney tissue itself on the microscopic level (76).

Third, hepatocyte hypertrophy was assessed as it was expected that hepatic congestion causes cell swelling, which results in a lower cell nucleus to cell surface ratio after VCI constriction as cell surface increases. However, the presented project showed no difference in this ratio between sham-operated and VCI-constricted rats. This could be explained by the observation that liver congestion was limited after VCI constriction as normalized liver weight was not significantly increased in VCI-constricted rats. On the other hand, as increased bilirubin levels could indicate hepatocyte necrosis (as explained in 4.4.3), hepatocyte hypertrophy could be masked by a shrinking of necrotic cells leading to a higher cell nucleus to cell surface ratio. Consequently, it could be a next goal to specifically measure necrosis in liver tissue to confirm this theory.

4.6 Influence of abdominal congestion on fibrosis

As fibrogenesis in heart, kidney and liver tissues are detrimental for the functioning of these organs, it was investigated how an increase in abdominal CVP affected the percentage fibrosis in these organs (Figure 17). First, the heart was expected to have an increased level of fibrosis after VCI constriction. In heart failure, compensatory mechanisms are activated to preserve CO, which results in cardiac hypertrophy. This is accompanied by fibrosis and eventually impaired contractility (79). However, no changes were demonstrated in the percentage cardiac fibrosis after VCI constriction. This confirms the observation that VCI constriction had no effect on contractility as determined via the hemodynamic measurements in the LV, CO as measured via echocardiographic

parameters and cardiac wall thickness. This emphasizes the coherence of the presented results on the microscopic and functional level that VCI constriction did not affect heart function.

Second, a transition of tubular epithelial to myofibroblast phenotype in the kidney was considered as a response to RAAS activation. This can be seen as an adaptation to escape cell death, but with the expense of a phenotypic change. It is mainly angiotensin II that stimulates fibrogenesis via stimulation of extracellular matrix production in these myofibroblasts, but also via inhibition of matrix degeneration proteins (83). Consequently, as VCI constriction was expected to stimulate RAAS activation, an increase in the percentage renal fibrosis was predicted in VCI-constricted rats. As shown by the standard clinical tests, the effect of VCI constriction on kidney function was limited, but an increase in the width of Bowman's space was demonstrated on microscopic level. This difference in results was explained by the enormous reserve capacity of the kidney, which leads to changes on the microscopic level but maintains kidney function. Still, the percentage fibrosis was not increased, which may be the consequence of a too short follow-up period in order to develop a myofibroblast phenotype in tubular epithelial cells.

Third, hepatic fibrosis was considered as a consequence of chronic passive congestion after VCI constriction. Giallourakis *et al*. (2002) described the pattern of fibrosis generated by congestive heart failure (cardiac fibrosis) as different from other liver diseases. In cardiac fibrosis, there are stromal fibrotic bands of collagen that radiate outward from the blood vessels and eventually reach adjacent blood vessels. This was also seen in the presented project (indicated by green arrows in Figure 19) (84). It was already shown by Akiyoshi *et al*. (1998) that a VCI constriction of six weeks in male Wister rats between the diaphragm and the liver leads to fibrosis in the congestive liver (85). D'Amico *et al*. (2012) showed also in male Sprague-Dawley rats that the percentage fibrosis increases from 3 to 7% fibrosis in a model of portal hypertension (86). Although there are differences with these studies, similar results were obtained in the presented project after VCI constriction.

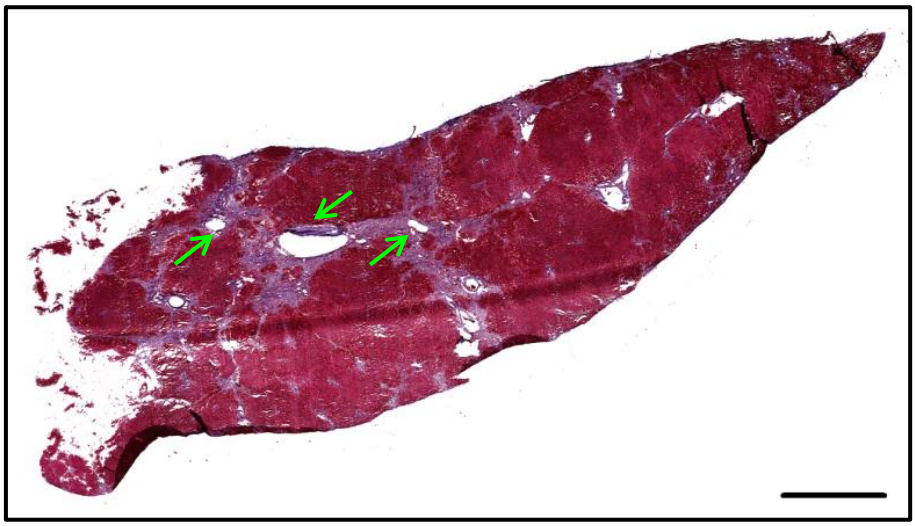

Figure 19: This is an example of a paraffin-embedded liver tissue section stained with Masson's trichrome of a VCI-constricted rat with cardiac fibrosis. A fibrotic radiation pattern is visible from different blood vessels (indicated with a green arrow).

Moreover, a positive correlation was found between plasma bilirubin levels and the percentage hepatic fibrosis (Figure 18). The increase in bilirubin levels is due to reduced hepatic excretion in the bile. This is explained by a change in the composition of the extracellular matrix in the liver due to fibrogenesis, contributing to a decreased exchange of bilirubin between hepatocytes, blood and bile. Hepatic fibrogenesis is mostly a reaction to persistent hepatocyte damage and necrosis (87). Therefore, it could be hypothesized that VCI constriction leads to hepatocyte necrosis (as suggested by an absence of hepatocyte hypertrophy), resulting in fibrosis and eventually increased bilirubin levels. Taken together, the liver is the only organ showing overt signs of deteriorating function and change in morphology after VCI constriction and seems to be the first target of VCI constriction. Although it may be suspected that also the spleen is one of the first targets as spleen weight normalized to tibia length was increased in VCI-constricted rats. However, this organ was not evaluated in the presented project, but could be included in future projects to complete the analysis on the targets of VCI constriction in the abdomen.

4.7 Limitations

First, the major limitation of this study is the disadvantages accompanied with the use of an animal model. There are interspecies differences, which complicates the extrapolation to human patients. On the other hand, genetic and environmental variations are present in humans while animals studies are completely standardized (57). Second, rat and human myocardium differ on several levels: a shorter action potential, a higher resting heart rate and regulation of calcium removal from the cytosol by the sarcoplasmic reticulum calcium pump (and not the sodium calcium exchanger) are present in rat myocardium (88, 89). This is not of great importance in the presented study as heart function was not affected by VCI constriction. Third, heart and kidney failure develop slowly, while in the rat the onset is forced. In humans, these failures are frequently encountered in the aging and older population, while young rats are used in studies (90). Fourth, IAP was not measured in the rats. As previously explained, IAP positively correlates to CVP, but directly measuring IAP in the rat would be advantageous to investigate the effect of IAP on heart and kidney function. However, by measuring the abdominal CVP an approximation of IAP is expected as a result. Last, the number of animals used in this project limits the power of the presented results as great variations were encountered. Therefore, it would be beneficial if a higher number of animals could be included, but this was limited in the presented studies due to practical reasons (e.g. limited number of metabolic cages).

4.8 Future perspectives

In the current project, a rat model of abdominal venous congestion is validated, but the effects of abdominal venous congestion on heart and kidney function were limited. As the short follow-up period of twelve weeks could account for the limited effects of VCI constriction on heart and kidney function, a longer study period will be included in following projects. The next goal will be to investigate RAAS activation, as this could explain the increase in cardiac contractility, plasma electrolytes and cys C levels. Moreover, cardiac and kidney biomarkers (as described in 1.3) will be measured to assess heart and kidney function more specifically. On the other hand, as fibrosis is already measured in heart, kidney and liver tissue sections, the precise pathways contributing to fibrosis will also be investigated in future research. The specific constituents of fibrosis will be

identified, including collagen I, III and IV. Moreover, transforming growth factor-β1 (TGF-β1) has been shown to induce transition of resident cells in the heart, kidneys and liver to α-smooth muscle actin (α-SMA)-expressing myofibrolast, which contribute to fibrosis (91-93). Therefore, the expression levels of TGF-β1, α-SMA and collagen I, III and IV determined by immunohistochemistry, western blotting and qPCR will demonstrate the precise mechanism through which fibrosis is induced in the heart, kidneys and liver. Additionally, spleen tissue could also be added to these analysis as the spleen is also a target of VCI constriction.

In future CRS research, the rat model of abdominal venous congestion can be used in combination with models of heart or kidney failure. This will clarify if abdominal venous congestion contributes to CRS progression and development. This combination will also provide a realistic analogy with CRS patients as they first present with heart or kidney failure before developing congestion. A next step will be to determine which part of the kidney tubule is affected most by abdominal venous congestion in the combined model. This objective will be investigated by administering different types of diuretics acting at different sites of the kidney tubule, including carbonic anhydrase, loop and thiazide diuretics directed at the proximal tubule, loop of Henle and distal tubule, respectively. Consequently, it will be possible to determine the best working diuretic, which will lead to treatment of CRS patients with more specific diuretics. This will maximize the reduction of abdominal congestion while minimizing worsening of renal function. On the other hand, the role of oxidative stress in heart and kidney damage can be investigated in CRS. It is expected that oxidative stress is also involved in the development and progression of CRS, since it has been shown that oxidative stress plays a role in heart and kidney failure separately (30). In this objective, dysfunctional ROS production and breakdown will be investigated, while the effects of ROS on DNA, proteins and lipids will be determined by measuring specific oxidative stress biomarkers. This knowledge will further contribute to the understanding on how the heart and kidneys are affected in CRS patients by oxidative stress.

To conclude, the knowledge obtained during the current and future projects can be further explored by pharmaceutical companies to develop new drugs (e.g. anti-fibrotic, optimized diuretic, anti-oxidant, etc.). This will result in more specific treatment regimens, shorter patients' hospital admission and less rehospitalization, which eventually will limit the costs for the patients and the society.

5 Conclusion

The objectives were to validate the rat model of abdominal venous congestion and to determine the effects of abdominal venous congestion on heart and kidney function. First, an increase in abdominal CVP and spleen weight was demonstrated, which are important determinants of abdominal venous congestion. Second, there was no effect of VCI constriction on heart function, which was confirmed by the echocardiographic analysis, CK activity levels, cardiac morphology and fibrosis. On the other hand, kidney function started to show signs of deterioration after VCI constriction. Plasma electrolytes and cys C levels and the width of Bowman's space were increased by the end of the follow-up period, but other clinical parameters (including GFR, FENa, urinary total protein and electrolytes) and the percentage fibrosis were unchanged after VCI constriction. This indicates that VCI constriction had an effect on kidney function, but the follow-up period limited the induction of overt kidney impairment. Last, liver function was also influenced by VCI constriction as bilirubin and the percentage fibrosis were increased after VCI constriction, which also showed a positive correlation. This further confirms the effect of VCI constriction on the abdomen. Based on the presented project, the liver was first targeted by abdominal venous congestion but the effect on the spleen should be further investigated.

Taken together, the rat model is validated as it is confirmed that VCI constriction induced abdominal venous congestion. However, the model in its present setup is not sufficient to induce CRS as heart and kidney function were minimally influenced by VCI constriction. To further investigate the role of abdominal venous congestion in CRS development and progression, it is suggested that future research uses a combination of this rat model with a model of heart or kidney failure. This combination has also the advantage of being in analogy with human patients.

6 References

1. Viswanathan G, Gilbert S. The cardiorenal syndrome: making the connection. International journal of nephrology. 2010.
2. Forman DE, Butler J, Wang Y, et al. Incidence, predictors at admission, and impact of worsening renal function among patients hospitalized with heart failure. Journal of the American College of Cardiology. 2004;43(1):61-7.
3. Adams KF, Fonarow GC, Emerman CL, et al. Characteristics and outcomes of patients hospitalized for heart failure in the United States: rationale, design, and preliminary observations from the first 100,000 cases in the Acute Decompensated Heart Failure National Registry (ADHERE). American heart journal. 2005;149(2):209-16.
4. Mozaffarian D, Benjamin EJ, Go AS, et al. Heart disease and stroke statistics-2015 update: a report from the american heart association. Circulation. 2015;131(4):e29.
5. Dickstein K, Cohen-Solal A, Filippatos G, et al. ESC Guidelines for the diagnosis and treatment of acute and chronic heart failure 2008‡. European journal of heart failure. 2008;10(10):933-89.
6. Ronco C, McCullough P, Anker SD, et al. Cardio-renal syndromes: report from the consensus conference of the acute dialysis quality initiative. European heart journal. 2010;31(6):703-11.
7. Du Y, Li X, Liu B. Advances in pathogenesis and current therapeutic strategies for cardiorenal syndrome. Life sciences. 2014;99(1):1-6.
8. Tang WW, Mullens W. Cardiorenal syndrome in decompensated heart failure. Heart. 2010;96(4):255-60.
9. Mullens W, Abrahams Z, Francis GS, et al. Importance of venous congestion for worsening of renal function in advanced decompensated heart failure. Journal of the American College of Cardiology. 2009;53(7):589-96.
10. Winton F. The influence of venous pressure on the isolated mammalian kidney. The Journal of physiology. 1931;72(1):49-61.
11. Mullens W, Abrahams Z, Skouri HN, et al. Elevated intra-abdominal pressure in acute decompensated heart failure: a potential contributor to worsening renal function? Journal of the American College of Cardiology. 2008;51(3):300-6.
12. Nijst P, Mullens W. The Acute Cardiorenal Syndrome: Burden and Mechanisms of Disease. Current heart failure reports. 2014;11(4):453-62.
13. Mullens W, Abrahams Z, Francis GS, et al. Prompt reduction in intra-abdominal pressure following large-volume mechanical fluid removal improves renal insufficiency in refractory decompensated heart failure. Journal of cardiac failure. 2008;14(6):508-14.
14. Kirkpatrick AW, Roberts DJ, De Waele J, et al. Intra-abdominal hypertension and the abdominal compartment syndrome: updated consensus definitions and clinical practice guidelines from the World Society of the Abdominal Compartment Syndrome. Intensive care medicine. 2013;39(7):1190-206.
15. Verbrugge FH, Dupont M, Steels P, et al. Abdominal contributions to cardiorenal dysfunction in congestive heart failure. Journal of the American College of Cardiology. 2013;62(6):485-95.
16. Valenza F, Chevallard G, Porro GA, et al. Static and dynamic components of esophageal and central venous pressure during intra-abdominal hypertension*. Critical care medicine. 2007;35(6):1575-81.
17. Küntscher MV, Germann G, Hartmann B. Correlations between cardiac output, stroke volume, central venous pressure, intra-abdominal pressure and total circulating blood volume in resuscitation of major burns. Resuscitation. 2006;70(1):37-43.
18. Bradley SE, Bradley GP. The effect of increased intra-abdominal pressure on renal function in man. Journal of Clinical Investigation. 1947;26(5):1010.
19. Doty JM, Saggi BH, Sugerman HJ, et al. Effect of increased renal venous pressure on renal function. Journal of Trauma and Acute Care Surgery. 1999;47(6):1000.
20. Greenway C, Lister G. Capacitance effects and blood reservoir function in the splanchnic vascular bed during non-hypotensive haemorrhage and blood volume expansion in anaesthetized cats. The Journal of physiology. 1974;237(2):279-94.
21. Fallick C, Sobotka PA, Dunlap ME. Sympathetically mediated changes in capacitance redistribution of the venous reservoir as a cause of decompensation. Circulation: Heart Failure. 2011;4(5):669-75.
22. Ming Z, Smyth DD, Lautt WW. Decreases in portal flow trigger a hepatorenal reflex to inhibit renal sodium and water excretion in rats: role of adenosine. Hepatology. 2002;35(1):167-75.
23. Garnett E, Goddard B, Markby D, et al. The spleen as an arteriovenous shunt. The Lancet. 1969;293(7591):386-8.
24. Sandek A, Bauditz J, Swidsinski A, et al. Altered intestinal function in patients with chronic heart failure. Journal of the American College of Cardiology. 2007;50(16):1561-9.
25. Charalambous BM, Stephens RC, Feavers IM, et al. Role of bacterial endotoxin in chronic heart failure: the gut of the matter. Shock. 2007;28(1):15-23.
26. Cullen DJ, Coyle JP, Teplick R, et al. Cardiovascular, pulmonary, and renal effects of massively increased intra-abdominal pressure in critically ill patients. Critical care medicine. 1989;17(2):118-21.
27. Epstein FH, Schrier RW, Abraham WT. Hormones and hemodynamics in heart failure. New England Journal of Medicine. 1999;341(8):577-85.
28. Heymes C, Bendall JK, Ratajczak P, et al. Increased myocardial NADPH oxidase activity in human heart failure. Journal of the American College of Cardiology. 2003;41(12):2164-71.
29. Vaziri ND, Dicus M, Ho ND, et al. Oxidative stress and dysregulation of superoxide dismutase and NADPH oxidase in renal insufficiency. Kidney international. 2003;63(1):179-85.
30. Rubattu S, Mennuni S, Testa M, et al. Pathogenesis of chronic cardiorenal syndrome: is there a role for oxidative stress? International journal of molecular sciences. 2013;14(11):23011-32.

31. McMurray JJ, Adamopoulos S, Anker SD, et al. ESC Guidelines for the diagnosis and treatment of acute and chronic heart failure 2012. European journal of heart failure. 2012;14(8):803-69.
32. Morrow DA, de Lemos JA. Benchmarks for the assessment of novel cardiovascular biomarkers. Circulation. 2007;115(8):949-52.
33. Cruz DN, Goh CY, Palazzuoli A, et al. Laboratory parameters of cardiac and kidney dysfunction in cardio-renal syndromes. Heart failure reviews. 2011;16(6):545-51.
34. Bennett M, Dent CL, Ma Q, et al. Urine NGAL predicts severity of acute kidney injury after cardiac surgery: a prospective study. CLINICAL JOURNAL-AMERICAN SOCIETY OF NEPHROLOGY. 2008;3(3):665.
35. Nguyen MT, Devarajan P. Biomarkers for the early detection of acute kidney injury. Pediatric nephrology. 2008;23(12):2151-7.
36. Poniatowski B, Malyszko J, Bachorzewska-Gajewska H, et al. Serum neutrophil gelatinase-associated lipocalin as a marker of renal function in patients with chronic heart failure and coronary artery disease. Kidney and Blood Pressure Research. 2009;32(2):77-80.
37. Soto K, Coelho S, Rodrigues B, et al. Cystatin C as a marker of acute kidney injury in the emergency department. Clinical Journal of the American Society of Nephrology. 2010;5(10):1745-54.
38. Ichimura T, Bonventre JV, Bailly V, et al. Kidney injury molecule-1 (KIM-1), a putative epithelial cell adhesion molecule containing a novel immunoglobulin domain, is up-regulated in renal cells after injury. Journal of Biological Chemistry. 1998;273(7):4135-42.
39. Liangos O, Perianayagam MC, Vaidya VS, et al. Urinary N-acetyl-β-(D)-glucosaminidase activity and kidney injury molecule-1 level are associated with adverse outcomes in acute renal failure. Journal of the American Society of Nephrology. 2007;18(3):904-12.
40. Wu B, Jiang H, Lin R, et al. Pretreatment with B-type natriuretic peptide protects the heart from ischemia-reperfusion injury by inhibiting myocardial apoptosis. The Tohoku journal of experimental medicine. 2009;219(2):107-14.
41. D'souza S, Baxter G. B Type natriuretic peptide: a good omen in myocardial ischaemia? Heart. 2003;89(7):707-9.
42. Fonarow GC, Peacock WF, Phillips CO, et al. Admission B-type natriuretic peptide levels and in-hospital mortality in acute decompensated heart failure. Journal of the American College of Cardiology. 2007;49(19):1943-50.
43. Lee SR, Jeong KH. Novel biomarkers for cardio-renal syndrome. Electrolytes & Blood Pressure. 2012;10(1):12-7.
44. Gordon A, Homsher E, Regnier M. Regulation of contraction in striated muscle. Physiological reviews. 2000;80(2):853-924.
45. Apple FS, Murakami MM, Pearce LA, et al. Predictive value of cardiac troponin I and T for subsequent death in end-stage renal disease. Circulation. 2002;106(23):2941-5.
46. Verbrugge FH, Grieten L, Mullens W. New insights into combinational drug therapy to manage congestion in heart failure. Current heart failure reports. 2014;11(1):1-9.
47. Kim G-H. Long-term adaptation of renal ion transporters to chronic diuretic treatment. American journal of nephrology. 2004;24(6):595-605.
48. Hasselblad V, Stough WG, Shah MR, et al. Relation between dose of loop diuretics and outcomes in a heart failure population: results of the ESCAPE trial. European journal of heart failure. 2007;9(10):1064-9.
49. Loon NR, Wilcox CS, Unwin RJ. Mechanism of impaired natriuretic response to furosemide during prolonged therapy. Kidney Int. 1989;36(4):682-9.
50. Schnermann J. Juxtaglomerular cell complex in the regulation of renal salt excretion. American Journal of Physiology-Regulatory, Integrative and Comparative Physiology. 1998;274(2):R263-R79.
51. Ali SS, Olinger CC, Sobotka PA, et al. Loop diuretics can cause clinical natriuretic failure: a prescription for volume expansion. Congestive Heart Failure. 2009;15(1):1-4.
52. Bart BA, Goldsmith SR, Lee KL, et al. Ultrafiltration in decompensated heart failure with cardiorenal syndrome. New England Journal of Medicine. 2012;367(24):2296-304.
53. Koch M, Haastert B, Kohnle M, et al. Peritoneal dialysis relieves clinical symptoms and is well tolerated in patients with refractory heart failure and chronic kidney disease. European journal of heart failure. 2012;14(5):530-9.
54. McKie PM, Schirger JA, Costello-Boerrigter LC, et al. Impaired natriuretic and renal endocrine response to acute volume expansion in pre-clinical systolic and diastolic dysfunction. Journal of the American College of Cardiology. 2011;58(20):2095-103.
55. Costanzo MR, Heywood JT, Massie BM, et al. A double-blind, randomized, parallel, placebo-controlled study examining the effect of cross-linked polyelectrolyte in heart failure patients with chronic kidney disease. European journal of heart failure. 2012;14(8):922-30.
56. Henderson LW, Dittrich HC, Strickland A, et al. A Phase 1 dose-ranging study examining the effects of a superabsorbent polymer (CLP) on fluid, sodium and potassium excretion in healthy subjects. BMC Pharmacology and Toxicology. 2014;15(1):1-7.
57. Bongartz LG, Braam B, Gaillard CA, et al. Target organ cross talk in cardiorenal syndrome: animal models. American Journal of Physiology-Renal Physiology. 2012;303(9):F1253-F63.
58. Meier C, Contaldo C, Schramm R, et al. A new model for the study of the abdominal compartment syndrome in rats. Journal of Surgical Research. 2007;139(2):209-16.
59. Paganelli WC, Cant JR, Pintal RR, et al. Plasma atrial natriuretic factor during chronic thoracic inferior vena caval constriction. Circulation research. 1988;62(2):279-85.
60. Neal Anjan Chatterjee MAF. Pathophysiology of heart diseases. fifth ed2011.
61. Huang H, Shan J, Pan X-H, et al. Carvedilol improved diabetic rat cardiac function depending on antioxidant ability. Diabetes research and clinical practice. 2007;75(1):7-13.

62. Lala A, McNulty SE, Mentz RJ, et al. Relief and recurrence of congestion during and after hospitalization for acute heart failure: insights from DOSE-AHF and CARRESS-HF. Circulation: Heart Failure. 2015:CIRCHEARTFAILURE. 114.001957.
63. Watson LE, Sheth M, Denyer RF, et al. Baseline echocardiographic values for adult male rats. Journal of the American Society of Echocardiography. 2004;17(2):161-7.
64. Lippi G, Luca Salvagno G, Montagnana M, et al. Influence of hemolysis on routine clinical chemistry testing. Clinical Chemical Laboratory Medicine. 2006;44(3):311-6.
65. Du Q, Hao C, Gou J, et al. Protective effects of p-nitro caffeic acid phenethyl ester on acute myocardial ischemia-reperfusion injury in rats. Experimental and Therapeutic Medicine. 2016;11(4):1433-40.
66. Ingwall JS. Energy metabolism in heart failure and remodelling. Cardiovascular research. 2009;81(3):412-9.
67. Gunst JJ, Langlois MR, Delanghe JR, et al. Serum creatine kinase activity is not a reliable marker for muscle damage in conditions associated with low extracellular glutathione concentration. Clinical chemistry. 1998;44(5):939-43.
68. Radovanovic S, Savic-Radojevic A, Pljesa-Ercegovac M, et al. Markers of oxidative damage and antioxidant enzyme activities as predictors of morbidity and mortality in patients with chronic heart failure. Journal of cardiac failure. 2012;18(6):493-501.
69. Ashtiyani SC, Najafi H, Jalalvandi S, et al. Protective effects of Rosa canina L fruit extracts on renal disturbances induced by reperfusion injury in rats. Iranian journal of kidney diseases. 2013;7(4):290.
70. Damman K, van Deursen VM, Navis G, et al. Increased central venous pressure is associated with impaired renal function and mortality in a broad spectrum of patients with cardiovascular disease. Journal of the American College of Cardiology. 2009;53(7):582-8.
71. Dharnidharka VR, Kwon C, Stevens G. Serum cystatin C is superior to serum creatinine as a marker of kidney function: a meta-analysis. American Journal of Kidney Diseases. 2002;40(2):221-6.
72. Uzun H, Keles MO, Ataman R, et al. Serum cystatin C level as a potentially good marker for impaired kidney function. Clinical biochemistry. 2005;38(9):792-8.
73. Efrati S, Berman S, Hamad RA, et al. Effect of captopril treatment on recuperation from ischemia/reperfusion-induced acute renal injury. Nephrology Dialysis Transplantation. 2011:gfr256.
74. Kim S, Yang JY, Jung ES, et al. Effects of sodium citrate on salt sensitivity and kidney Injury in chronic renal failure. Journal of Korean medical science. 2014;29(12):1658-64.
75. Regeniter A, Siede WH, Scholer A, et al. Interpreting complex urinary patterns with MDI LABLINK: a statistical evaluation. Clinica chimica acta. 2000;297(1):261-73.
76. Liu KD, Brakeman PR. Renal repair and recovery. Critical care medicine. 2008;36(4):S187-S92.
77. Sticova E, Jirsa M. New insights in bilirubin metabolism and their clinical implications. World J Gastroenterol. 2013;19(38):6398-407.
78. Van Deursen V, Damman K, Hillege H, et al. Abnormal liver function in relation to hemodynamic profile in heart failure patients. Journal of cardiac failure. 2010;16(1):84-90.
79. Kemp CD, Conte JV. The pathophysiology of heart failure. Cardiovascular Pathology. 2012;21(5):365-71.
80. Sunagawa Y, Sono S, Katanasaka Y, et al. Optimal Dose-Setting Study of Curcumin for Improvement of Left Ventricular Systolic Function After Myocardial Infarction in Rats. Journal of pharmacological sciences. 2014;126(4):329-36.
81. Dilley JR, Corradi A, Arendshorst WJ. Glomerular ultrafiltration dynamics during increased renal venous pressure. American Journal of Physiology-Renal Physiology. 1983;244(6):F650-F8.
82. Kotyk T, Dey N, Ashour AS, et al. Measurement of the Glomerulus Diameter and Bowman's Space Thickness of Renal Albino Rats. Computer Methods and Programs in Biomedicine. 2015.
83. Burns W, Thomas M. Angiotensin II and its role in tubular epithelial to mesenchymal transition associated with chronic kidney disease. Cells Tissues Organs. 2010;193(1-2):74-84.
84. Giallourakis CC, Rosenberg PM, Friedman LS. The liver in heart failure. Clinics in liver disease. 2002;6(4):947-67.
85. Akiyoshi H, Terada T. Centrilobular and perisinusoidal fibrosis in experimental congestive liver in the rat. Journal of hepatology. 1999;30(3):433-9.
86. D'Amico M, Mejías M, García-Pras E, et al. Effects of the combined administration of propranolol plus sorafenib on portal hypertension in cirrhotic rats. American Journal of Physiology-Gastrointestinal and Liver Physiology. 2012;302(10):G1191-G8.
87. Pinzani M, Rombouts K. Liver fibrosis: from the bench to clinical targets. Digestive and liver disease. 2004;36(4):231-42.
88. Bers DM. Cardiac Na/Ca exchange function in rabbit, mouse and man: what's the difference? Journal of molecular and cellular cardiology. 2002;34(4):369-73.
89. Endoh M. Force–frequency relationship in intact mammalian ventricular myocardium: physiological and pathophysiological relevance. European journal of pharmacology. 2004;500(1):73-86.
90. Doggrell SA, Brown L. Rat models of hypertension, cardiac hypertrophy and failure. Cardiovascular research. 1998;39(1):89-105.
91. Leslie K, Taatjes D, Schwarz J. Cardiac myofibroblasts express alpha smooth muscle actin during right ventricular pressure overload in the rabbit. The American journal of pathology. 1991;139(1):207.
92. Masszi A, Di Ciano C, Sirokmány G, et al. Central role for Rho in TGF-β1-induced α-smooth muscle actin expression during epithelial-mesenchymal transition. American Journal of Physiology-Renal Physiology. 2003;284(5):F911-F24.
93. Schmitt-Gräff A, Krüger S, Bochard F, et al. Modulation of alpha smooth muscle actin and desmin expression in perisinusoidal cells of normal and diseased human livers. The American journal of pathology. 1991;138(5):1233.

Auteursrechtelijke overeenkomst

Ik/wij verlenen het wereldwijde auteursrecht voor de ingediende eindverhandeling:
Characterization of a new rat model for the cardio-renal syndrome

Richting: **master in de biomedische wetenschappen-klinische moleculaire wetenschappen**
Jaar: **2016**

in alle mogelijke mediaformaten, - bestaande en in de toekomst te ontwikkelen - , aan de Universiteit Hasselt.

Niet tegenstaand deze toekenning van het auteursrecht aan de Universiteit Hasselt behoud ik als auteur het recht om de eindverhandeling, - in zijn geheel of gedeeltelijk -, vrij te reproduceren, (her)publiceren of distribueren zonder de toelating te moeten verkrijgen van de Universiteit Hasselt.

Ik bevestig dat de eindverhandeling mijn origineel werk is, en dat ik het recht heb om de rechten te verlenen die in deze overeenkomst worden beschreven. Ik verklaar tevens dat de eindverhandeling, naar mijn weten, het auteursrecht van anderen niet overtreedt.

Ik verklaar tevens dat ik voor het materiaal in de eindverhandeling dat beschermd wordt door het auteursrecht, de nodige toelatingen heb verkregen zodat ik deze ook aan de Universiteit Hasselt kan overdragen en dat dit duidelijk in de tekst en inhoud van de eindverhandeling werd genotificeerd.

Universiteit Hasselt zal mij als auteur(s) van de eindverhandeling identificeren en zal geen wijzigingen aanbrengen aan de eindverhandeling, uitgezonderd deze toegelaten door deze overeenkomst.

Voor akkoord,

Blockken, Laura

Datum: **7/06/2016**